NUMERICAL ANALYSIS OF LAVA COOLING WITH DIFFERENT GEOMETRIC CONFIGURATIONS

Prepared for

U.S. Nuclear Regulatory Commission
Contract Nos. NRC–02–07–006 and NRC–HQ–12–C–02–0089

Prepared by

Debashis Basu[1]
Kaushik Das[1]
Stephen Self[2]

[1]Center for Nuclear Waste Regulatory Analyses
San Antonio, Texas

[2]U.S. Nuclear Regulatory Commission
Washington, DC

September 2013

ABSTRACT

This report documents the results of a numerical analysis carried out to understand the cooling of lava flows in an external open environment using the computational fluid dynamics code/program ANSYS® FLUENT™ Version 12.1 (ANSYS, Inc., 2009) and 14.0 (ANSYS, Inc., 2011). Simulations were initialized using ANSYS FLUENT Version 12.1, but subsequently the version was upgraded to Version 14.0. The report also describes the generic problem of heat transfer and cooling patterns among multiple hot bodies, which has relevance to both natural and engineered barrier systems. This work is a continuation of previous work (Basu, et al., 2012) that focused on cooling of a single lobe. In the present work, different temporal configurations are considered for the case of two tabular bodies of lava cooling together with a cooler (previously emplaced) lobe at the bottom and a hotter lobe on top. The cooling of the pair of lobes along with the thermal characteristics of the lobe pair is analyzed. For the present analysis, the Navier-Stokes equations are solved in two dimensions. The lava and its surroundings are modeled as two-dimensional elements effectively forming extensive stacked layers on top of each other, with no heat transfer from the two vertical sides considered in the simulations. Heat transfer is considered only from the top surface and in the contact zone between the two lobes.

The present analysis focused on predicting the cooling behavior and pattern when an extensive hot lobe {maximum emplacement temperature of 1,500 K [2,240 °F] } is placed on top of an extensive, older, still-cooling lobe. Two different configurations have been considered. In the first configuration, the bottom lobe has cooled under ambient surface conditions for 3 months (time elapsed after emplacement), while the upper has cooled under ambient conditions for 1 month before it is introduced onto the lower lobe. In the second configuration, the bottom lobe has cooled under ambient conditions for 12 months, while the upper lobe has cooled for 1 month (as described previously). The geometric configuration is such that the lower crust of the upper lobe in the previously simulated single lava lobe is not considered in the simulations. The top lobe has essentially the upper crust of a previously simulated single lava lobe (Basu, et al., 2012) after the cooling time indicated (1 month). Similarly the bottom lobe is essentially the full lower and upper crust of a previously simulated single lava lobe (Basu, et al., 2012) after the cooling time indicated (3 months and 12 months for the 2 different temporal configurations). Movement of air (wind) is not modeled but is accommodated by keeping the ambient atmospheric temperature at 305 K [90 °F]. The heat transfer between the top surface of the upper lobe and the atmosphere is assumed to be controlled by convective heat transfer and radiation. Simulations for both configurations are conducted with constant lava viscosity, constant thermal conductivity, and constant density and are under the influence of simulated heat loss due to rainfall. Heat flow transport from the lava to its surroundings is modeled through radiation and convection from the surface of the lobe(s) as well as through conduction to the ground. Internally, a conduction-only approach moves heat from the interior outward. Simulation parameters for the lava properties are obtained from a previous numerical study on lava cooling after the 1997 Okmok (Alaska) eruption (Patrick, et al., 2004).

Simulations were carried out for a computational time equivalence of up to 6 years. Computed results show that the lava temperature for the lower cooler lobe increases after contact with the new hot lobe at the top. A significant increase in temperature in the mid-section (where the two lobes join together) is observed, even after the lower lobe was allowed to cool for 1 year. However, the maximum heating of the top of the lower lobe in the mid-section occurs within the first 3 years and drops off afterwards. Heat conduction takes place almost to the lower crust of the lower lobe. The upper crust of the lower lobe increases in temperature; the lower crust is affected little during a 6-year period. For the upper lobe, at the uppermost crust (in contact with

the ambient surface conditions) the temperature drop is, of course, much more significant and cools by approximately 300 K [540°F] at a depth of ~12 m [40 ft] in the same 6-year period. This is expected because the starting temperature for the upper lobe is significantly higher than that of the lower lobe and the upper lobe is exposed to the atmosphere and rain for a longer time.

Potential future applications for this type of simulation include the cooling of hot nuclear waste canisters emplaced in a warm borehole.

REFERENCES

ANSYS, Inc. "ANSYS FLUENT Version 14.0, User's Guide." Canonsburg, Pennsylvania: ANSYS, Inc. 2011.

_____. "ANSYS FLUENT Version 12.1, User's Guide." Canonsburg, Pennsylvania: ANSYS, Inc. 2009.

Basu, D., K. Das, and S. Self. "Numerical Simulations and Analysis of Lava Flow Cooling." San Antonio, Texas: Center for Nuclear Waste Regulatory Analyses. February 2012.

Patrick, M.R., J. Dehn, and K. Dean. "Numerical Modeling of Lava Flow Cooling Applied to the 1997 Okmok Eruption: Approach and Analysis." *Journal of Geophysical Research*. Vol. 109. 2004.

CONTENTS

FIGURES

FIGURES (continued)

Figures Page

TABLES

ACKNOWLEDGMENTS

This report describes work performed by the Center for Nuclear Waste Regulatory Analyses (CNWRA®) for the U.S. Nuclear Regulatory Commission (NRC) under Contract Nos. NRC–02–07–006 and NRC–HQ–12–C–02–0089. The activities reported here were performed on behalf of the NRC Office of Nuclear Material Safety and Safeguards, Division of Spent Fuel Alternative Strategies. This report is an independent product of CNWRA and does not necessarily reflect the view or regulatory position of NRC. The NRC staff views expressed herein are preliminary and do not constitute a final judgment or determination of the matters addressed or of the acceptability of any licensing action that may be under consideration at NRC.

The authors gratefully acknowledge D. Hooper for his technical review, E. Pearcy and G. Wittmeyer for their programmatic reviews, L. Mulverhill for her editorial review, and A. Ramos for his administrative support. M. Elyyan from ANSYS Company is also acknowledged for his advice and help in setting up the simulation cases used in this study.

QUALITY OF DATA, ANALYSES, AND CODE DEVELOPMENT

DATA: All CNWRA-generated original data contained in this report meet quality assurance requirements described in the Geosciences and Engineering Division Quality Assurance Manual. Sources of other data should be consulted for determining the level of quality of those data. The work presented in this report is documented in Scientific Notebook No. 1114E (Basu and Das, 2012).

ANALYSES AND CODES: The general purpose computational fluid dynamics simulation code ANSYS® FLUENT™ Versions 12.1 (ANSYS, Inc., 2009) and 14.0 (ANSYS, Inc. 2011) was used to generate results for this report and is controlled in accordance with the CNWRA Technical Operating Procedure (TOP)–018, Development and Control of Scientific and Engineering Software. All postprocessing was done using TECPLOT® 360™ Version 2009 (TECPLOT, Inc., 2009). The simulations were initiated with ANSYS® FLUENT™ Version 12.1 and later switched to ANSYS® FLUENT™ Version 14.0 to utilize the capabilities of a newer version of this software.

References

ANSYS, Inc. "ANSYS FLUENT Version 14.0, User's Guide." Canonsburg, Pennsylvania: ANSYS, Inc. 2011.

_____. "ANSYS FLUENT Version 12.1, User's Guide." Canonsburg, Pennsylvania: ANSYS, Inc. 2009.

Basu, D. and K. Das. "Numerical Simulation of Lava Cooling: ISFR-Task 2." Scientific Notebook No. 1114E. San Antonio, Texas: CNWRA. pp. 1–51. 2012.

TECPLOT, Inc. "TECPLOT 360 Version 2009." Bellevue, Washington: TECPLOT, Inc. 2009.

1 INTRODUCTION

This report describes work conducted as part of the NRC Disposal-Related Integrated Spent Nuclear Fuel Regulatory Activities program. The report provides previously undocumented results for recent numerical simulations for cooling of magma as a lava flow. It is a continuation of previous work by Basu, et al. (2012) that focused on cooling of a single 50-m [164-ft]-thick lobe of lava in the natural environment. This report presents results of simulations carried out to evaluate the dynamics involved in cooling multiple lava lobes stacked on top of each other with different temporal (thermal) configurations. These simulations were conducted to assess the cooling pattern of lava lobes after they become stagnant. The simulations employ a geometry that consists of two hot lava lobes (cooled to different time intervals) placed on top of each other. While the lower lava lobe is at a relatively cooler temperature (representing 3 months and 12 months of cooling before the upper lobe is placed upon it), the upper lava lobe is at a hotter temperature (represented by a similar-sized lobe that has been cooling for 1 month). The cooling of the pair of lobes, along with the thermal characteristics of the lobe pair, is analyzed. Computed results show that the lava temperature for the lower cooler lobe increases after contact with the new hot lobe at the top. A significant increase in temperature in the mid-section (where the two lobes join) is observed, even after the lower lobe was allowed to cool for 1 year before superposition of the upper lobe. However, the maximum heating of the top of the lower lobe in the mid-section occurs within the first 3 years and drops off afterwards.

The essence of the numerical analysis is related to the cooling of hot bodies in the natural environment (e.g., on the surface, influenced by wind and rain, or under the surface, influenced by existing bodies of hot lava, rock, and groundwater). The current study and analysis can be applied to any cooling hot body where conduction dominates internal heat loss, but radiation to, and convection in, the outside environment aids surface cooling. In addition, this analysis can be applied for heat transfer analysis when there is a significant temperature difference between two bodies on top of each other. Convection is not predicted to occur inside the hot body being considered (lava, in this case), but some results suggest that convection may occur under some circumstances. This work aims to assess the thermal characteristics of a lava lobe pair during cooling in a natural environment, accounting for variability within the environment during the time taken to cool to the ambient temperature. Part of the purpose of this modeling is to extend the computational fluid dynamics methodology applied to cooling of single lava lobes (Basu, et al., 2012) to a configuration involving multiple lava lobes of different thermal characteristics. Another objective of the current work is to investigate the effect of different bottom lobe cooling times (1 month versus 3 months' cooling before the upper lobe arrives) on the cooling history, temperature profiles and solidification of the lava pair. Simulations have been carried out using constant lava parameters, such as thermal conductivity and viscosity. Temperature-dependent thermal conductivity and viscosity have not been considered in the present analysis (see Basu, et al., 2012).

1.1 Background

Lava flow cooling has been an area of active research interest over the last few decades. Lavas develop cooled crusts while being emplaced; the upper crust is generally thicker than the lower in cooled lava units (Keszthelyi and Denlinger, 1996; Patrick, et al., 2004). Several researchers (Shaw, et al., 1977; Peck, et al., 1977; Keszthelyi and Denlinger, 1996; Neri, 1998; Keszthelyi, et al., 2003) have studied different aspects of lava cooling. Numerical simulations of lava cooling involve a number of assumptions for the different thermodynamic processes that influence the cooling process as well as the material properties that define the lava characteristics. Shaw, et al. (1977) and Peck, et al. (1977) developed one of the earliest

numerical models for lava flow cooling using a simplified approach whereby the ground and lava were modeled as a stack of elements and the top and bottom of the stack were maintained at a constant 273 K [32 °F]. The model accurately characterized the internal temperature of the Alae lava lake, Hawaii.

Keszthelyi and Denlinger (1996) developed a numerical model for lava cooling that included surface cooling by both thermal radiation and atmospheric convection. The developed model realistically predicted the cooling rates of pahoehoe flows under different conditions. Keszthelyi and Denlinger (1996) found that while thermal radiation is the dominant initial heat loss mechanism, atmospheric convective cooling also plays an important role, even in the initial cooling stages. The numerical approach Neri (1998) developed allowed the investigation of the main variables and parameters affecting the thermal-diffusion-dominated cooling process of a lava flow. The Neri (1998) approach also determined that surface features can strongly influence the global heat transfer between lava and atmosphere as well as the local cooling history of the flow. Keszthelyi, et al. (2003) used observational data to investigate the effect of wind speed on lava flow cooling. Comparison of the observed results to predictions from a wide range of convection formulas showed that (i) there is a general agreement between the predictions and observations and (ii) the effectiveness of free convection may have been underestimated in the past (Keszthelyi, et al., 2003). Several other past studies also addressed different aspects of lava cooling. These include Head and Wilson (1986), who looked at Venus flows; Ishihara, et al. (1990) and Dragoni (1989), who based their analyses on the assumption of radiation-dominated cooling; and Crisp and Baloga (1990), who characterized a'a lava surface heat losses. Young and Wadge (1990) developed a numerical program to model the path of flowing lava. Wooster, et al. (1997) carried out a detailed examination of the complete thermal budget of Etnean flows.

While the majority of the past work has focused on the characteristics of cooling lava by an analytical and semi-numerical approach, Basu, et al. (2012) used Navier-Stokes equations to carry out an extensive thermal analysis of the cooling of lava lobes under environmental conditions.

Basu, et al. (2012) systematically explored the importance of variable parameters on the predicted temperature field. Simulations were carried out with variable viscosity, constant viscosity, variable thermal conductivity, and variable density. The influence of the substrate underlying the hot lava body (consisting of carbonate rock overlain by a layer of previously solidified cold lava) on the cooling pattern was also analyzed. The analysis showed that the thermal field and solidification pattern varied significantly between simulations with a constant viscosity and those with a variable viscosity. Rayleigh-Taylor instabilities were observed with variable properties (thermal conductivity, density and viscosity). Rayleigh-Taylor instability takes a longer time to grow for more viscous fluid and smaller density difference. The general pattern of cooling and the thickness of lava crust developed {assessed by the ~1,173 K [1,652 °F] isotherm} obtained from these simulations are similar to those obtained by other simulation and observation, both modeled (Patrick, et al., 2004) and based on field measurements and an empirical model (Hon, et al., 1994). Temperatures in the range 1,173–1,273 K [1,652–1,832 °F] approximately mark the onset of viscoelastic behavior of cooling basaltic lava and thus indicate the innermost (hotter) parts of the upper and lower crusts {brittle behavior starts at ~1,073 K [1,472 °F]}. Therefore, the simulation of Basu, et al. (2012) provided a reasonable agreement with other estimates.

The present work is a continuation of the earlier work (Basu, et al., 2012), and the numerical methodology developed in the previous work has been extended to carry out the simulations for the lava lobe pair. Very little work has been done on the thermal interaction of adjacent lava lobes. The geometric configuration in this work is similar to the study Burkhard (2003) carried out on samples from thin, small pahoehoe lava lobes (toes). Burkhard did an experimental reheating analysis to investigate thermal interaction between two stacked, natural Hawaiian lava lobes, with an unknown time interval between the lobe emplacements. These thin {lower = 3 cm [1 in], upper = 7 cm [3 in]} glassy lobes must have cooled quickly. Results revealed that the cooled top of the bottom lobe {estimated to be <973 K [1,292 °F]} caused the top lobe to chill (without crystallization) to about 2 cm [0.8 in] from the contact and the arrival of the hot top lobe caused the previously glassy top of the lower lobe to recrystallize to a depth of ~1 cm [0.4 in]. Although this work does not specifically model crystallization with cooling, we do include the latent heat released by crystal growth in our scheme of the heat loss from hot lava.

In the present analysis we have modeled cooling in thick lava lobes and two different temperature profiles have been considered for the lower lobe. In one case, the lower lobe has a condition of 3 months' cooling, and in the other case, the lower lobe has a condition of 12 months' cooling before the top lobe is emplaced. As natural lava lobes thicken in place, for simplicity we have used a condition of 1 month's cooling at the time of emplacement of the top lobe over the bottom one and thus the start of the numerical experiments. Very little cooling and crust growth occurs in the first month (Basu, et al., 2012) and this starting condition permits us to model the thermal influence between two superposed, thick lobes.

The influence of wind is simulated through an ambient temperature boundary condition at the top surface. The air is assumed to be static with an ambient temperature and acts as a heat sink initially on the bottom lobe and then on the top lobe. Side cooling is ignored because our aim is to study the thermal behavior in extensive lava fields. The effect of heated air being transported away and subsequently replaced by colder air at the lobe tops is not directly considered in these simulations, but is accommodated by keeping the ambient temperature above the lobe constant. The computational models developed at the Center for Nuclear Waste Regulatory Analyses (CNWRA®) are based on some prior thermal analysis of lava cooling (Patrick, et al., 2004) carried out for flows produced during the 1997 Okmok, Alaska, eruption.

1.2 Purpose and Scope

This summary report documents the important technical aspects and results of computational analyses designed to investigate the cooling of hot lava lobes on the Earth's surface under different environmental conditions. The models are not designed to simultaneously simulate the flow of lava and its cooling, but rather the conditions when hot stagnant lava is cooling in contact with another lava lobe (e.g., previously partly solidified lava flow units that have cooled significantly). CNWRA staff conducted these numerical simulations to better understand and develop critical insights into the long-term (~3 years) thermal behavior of hot bodies in contact with a cooler body in natural conditions. Prior observations (Patrick, et al., 2004; Hon, et al., 1994) support this model because the model results are consistent with these observations.

Results presented in this report are compared to prior observations and measurements of lava cooling at actual volcano sites. To analyze the thermal field and evaluation of cooling, the work is restricted to two-dimensional numerical simulations under conditions of transient cooling analysis. No non-Newtonian viscosities, such as Bingham-Plastic, are assumed for the stagnant, cooling lava. Instead, values and correlations obtained from prior investigations

(Patrick, et al., 2004; Keszthelyi and Denlinger, 1996) involving viscosity and thermal conductivity of basaltic lavas are used in the current analysis.

The initial conditions for the simulations are obtained from the previously conducted simulations for cooling of individual lava lobes (Basu, et al., 2012). The geometric configuration is such that the lower crust of the upper lobe is not considered in the simulations. The top lobe has essentially the upper crust of the previously simulated single lava lobe (Basu, et al., 2012) after the cooling time indicated (1 month). This is adopted to enable us to simple model the arrival of a new lava lobe that has been extending and growing over a pre-existing lobe for some time before the desired simulation begins (at the point of stagnation of the upper lobe). Similarly the bottom lobe has essentially the lower crust of a previously simulated single lava lobe (Basu, et al., 2012) after the cooling time indicated (3 months and 12 months for the two different temporal configurations). Simulations were carried out for a computational time equivalence of 6 years. Based on the two-dimensional simulations, it was revealed that the lava crust temperature of the lower cooler lobe increases after contact with the new hot lobe at the top, as expected. A significant increase in temperature in the mid-section (at the point of contact of the two lobes) is observed, even after the lower lobe was allowed to cool for 1 year before the upper lobe was added. Using the two-dimensional simulations, salient features have been captured at a considerably reduced computational burden using the ANSYS® FLUENT™ Versions 12.1 (ANSYS, Inc., 2009) and 14.0 (ANSYS, Inc., 2011) computational fluid dynamics software package.

2 METHODOLOGY

2.1 Model Geometry

As noted earlier, the configuration modeled in this study is restricted to two dimensions. Figure 2-1 shows a 20- to 130-m [66- to 427-ft] computational domain used for the present computations. The configuration consists of a 50-m [164-ft]-thick, hot lava lobe at the top that has been cooled for 1 month before the simulations begin. Below the hot lava lobe, there is a second hot lava lobe 50 m [164 ft] thick, which had cooled for 3 months prior to superposition of the upper lobe and the start of the simulation. Below this is a substrate that consists of two parts: a layer of cooled, solidified lava 15 m [49 ft] in thickness, underlain by 15-m [49-ft]-thick cold ground (carbonate rock). The thicknesses are chosen based on the values Patrick, et al. (2004) used in similar prior calculations. The computational domain consists of a two-dimensional rectangular slab. A wide lava body of constant thickness has been considered in the current simulations. The edge effect is avoided by applying the periodic boundary condition. The geometry and schematic of the second configuration are shown in Figure 2-2.

The geometry of the configuration and the computational domain are provided in Table 2-1. The combined geometry is constructed using simulations previously carried out for individual lobes (Basu, et al., 2012). Once the simulation for the individual lobes is completed, the solutions at three different time intervals (1, 3, and 12 months) are used to generate the combined domain for the simulations. As mentioned in earlier sections, two combined configurations are considered: (i) the bottom lava lobe is cooled for 3 months before a 1-month-old lobe is emplaced on top and the solution initialized and (ii) the bottom lava lobe is cooled for 12 months before a 1-month-old lobe is emplaced on top and the solution initialized.

2.2 Computational Grid and Boundary Conditions

The two-dimensional uniform computational grid used in these simulations consists of 16,000 rectangular cells (Figure 2-3). Table 2-2 details the grid dimensions for each geometric construct. No clustering of the grid is employed near the wall regions. However, the computational grid in the vertical direction is clustered near the top boundary of the hot upper lobe and at the intersection of the hot lava with the substrate in the bottom lobe. This is done to efficiently capture the thermal gradients in those regions.

A periodic boundary condition is used in the horizontal *x* direction. The periodic boundary condition is used to implement the repetitiveness of the solution in the lateral direction. This boundary condition enables a more realistic simulation of an infinite length of a sheetlike lava body. In addition, no heat transfer is considered in the horizontal direction. For the top surface, a mixed convection–radiation boundary condition is used. Prior investigations (Keszthelyi and Denlinger, 1996; Neri, 1998; Keszthelyi, et al., 2003) demonstrated that heat transfer from the lava surface is dominated by both convection and radiation; hence we use a mixed boundary condition at the top. The heat transfer from the top is assumed to be taking place through the combination of convection and radiation, and the convective heat transfer coefficient, as well as the emissivity, is specified. Heat transfer between the hot lava and the cold lava substrate, and subsequently to the rock substrate layer, is through conductive heat transfer. The initial temperature is 1,500 K [2,240 °F] for the hot lava, while the substrate and the ground are

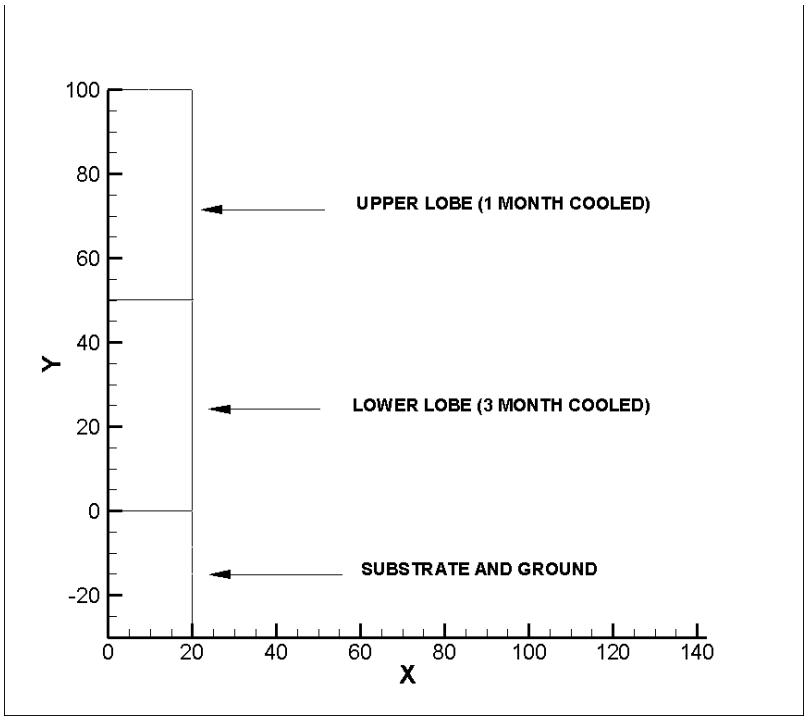

Figure 2-1. Schematic of the Model Configuration for the First Case Simulated; Length Is in Meters. Note that the Depth Into Substrate and Ground Is Indicated as a Negative Value.

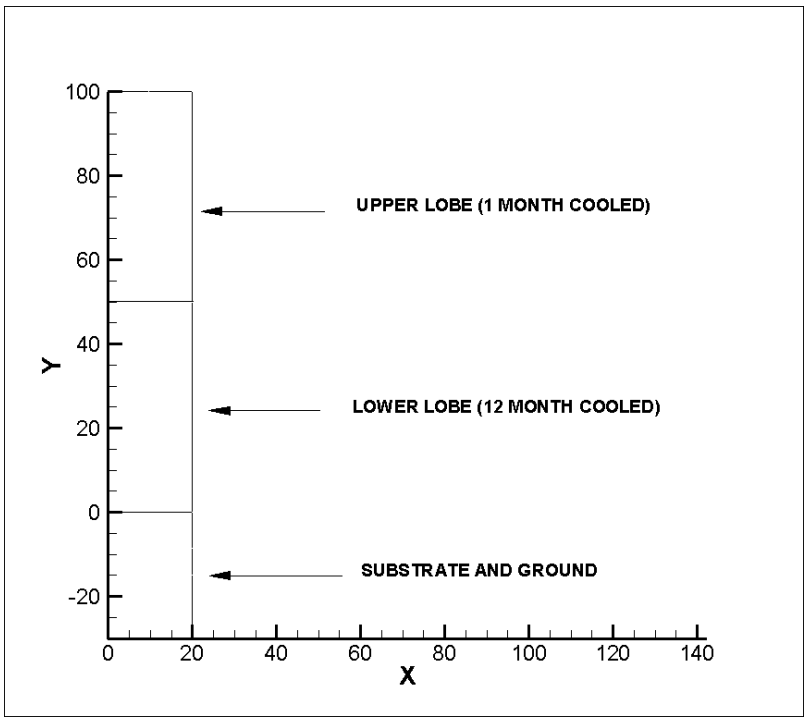

Figure 2-2. Schematic of the Model Configuration for the Second Case Simulated; Length Is in Meters. Note that the Depth Into Substrate and Ground Is Indicated as a Negative Value.

Table 2-1. Model Construct Values	
Construct	**Thickness Value**
Upper Lava Lobe (Cooled to 1 month)	50 m [164 ft]
Lower Lava Lobe (Cooled to 3 and 12 months)	50 m [164 ft]
• Substrate: Cold lava substrate (middle layer)	15 m [49 ft]
• Cold ground/rock (bottom layer)	15 m [49 ft]

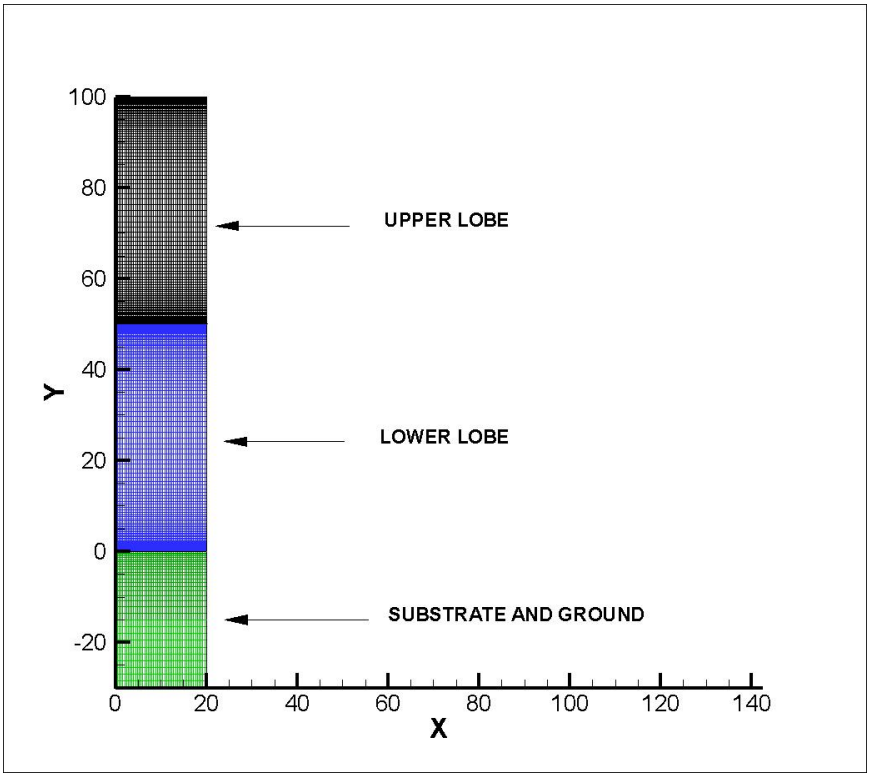

Figure 2-3. Schematic of the Computational Grid Used in the Simulations: Different Zones Are Shown in Different Colors and Length Is in Meters

Table 2-2. Details of the Computational Grid	
Construct	**Grid Dimension ($N_x \times N_y$)***
Hot lava thickness (at the top)	50 × 120
Cooled lava thickness (middle layer)	50 × 40
Cooled ground thickness (bottom layer)	30 × 40
*N_x = Number of cells in the x direction and N_y = number of cells in the y direction	

considered to be at a normal ambient temperature of 293 K [68 °F]. Starting with the initial lava temperature at 1,400 K [2,060 °F], similar to eruption temperatures of lavas at Kilauea, Hawaii, does not affect the scheme of cooling in the two lobes but lowers temperatures in the domain overall by ~373 K [671 °F].

The present simulations do not specifically take into account the wind velocity in the air above the hot lava. The effect of replacing warmed air above the hot lava body with colder air is

implemented through maintaining the ambient temperature at 305 K [89 °F]. The heat transfer between the top surface of the hot lava and the atmosphere is assumed to be controlled by the convective heat transfer and the radiation parameters. Prior investigations on external cooling of lava flows (Neri, 1998; Keszthelyi, et al., 2003) determined that in the initial stages of cooling there exists a substantial temperature difference between hot lava and the air above it. However, subsequent radiative heat loss quickly reduces the temperature of the lava top surface to values approaching those of the ambient temperature. The boundary conditions adopted in the present study are very similar to the boundary conditions adopted in the earlier study (Basu, et al., 2012). As explained in the next paragraph, the top surface is modeled as a heat sink to accommodate the effect of rainfall.

The effect of rainfall is essentially accommodated by increasing the heat loss per time. To simulate the effect of rainfall, the top surface boundary condition is changed to accommodate this condition. Patrick, et al. (2004) and Shaw, et al. (1977) detailed the effect of rainfall on the lava cooling. According to Patrick, et al. (2004), rain that contacts the hot upper surface will vaporize and extract heat from the flow at the top surface. The present set of computations with rainfall models the effect of rain through this latent heat of vaporization concept. This model with rain simulation is based on the prior observations by Shaw, et al. (1977). In their model, all rain contacting the top surface is assumed to vaporize completely. This enables the calculation of the latent heat of water vaporization in addition to a measurement of the heat required to raise the temperature of water from the ambient temperature value to 373 K [212 °F]. This total heat amount is subtracted from the top surface of the hot lava body. For all the computations, a rainfall flux of 0.04 gm/s/m^2 [8 × 10^{-5} lb/s/ft^2] is used. In the ANSYS-FLUENT model, the top surface is assigned as a heat sink, from where heat is extracted, in the simulation cases with rainfall.

The radiative heat transfer is calculated using the Stefan-Boltzmann equation [Eq. (2-1)]

$$Q_r = \sigma\varepsilon\,[T_h^4 - T_c^4] \qquad (2\text{-}1)$$

where σ is the Stefan-Boltzmann Constant given as 5.67 × 10^{-8} W m^{-2} K^{-4} [0.1714 × 10^{-8} BTU h^{-1} ft^{-2} R^{-4}]; ε is the emissivity for radiation and is taken as 0.95 in the present computations; T_h is the hot lava surface temperature; and T_c is the ambient temperature. The convective heat transfer is calculated through Newton's law of cooling. The value for the convective heat transfer coefficient is taken as 50 W/m^2 K [8.83 BTU h^{-1} ft^{-2} °F^{-1}].

2.3 Material Properties

Simulations are carried out for lava with constant properties. Lava property values are based on data available in the open literature (Keszthelyi and Denlinger, 1996; Neri, 1998; Keszthelyi, et al., 2003; Patrick, et al., 2004) and are listed in Table 2-3. These primarily are based on the values Patrick, et al. (2004) provided.

2.4 Numerical Methods

The commercial software ANSYS FLUENT was used for the simulations, which were initiated with ANSYS FLUENT Version 12.1 (ANSYS, Inc., 2009) and later switched to ANSYS FLUENT Version 14.0 (ANSYS, Inc., 2011). There are no significant changes between the two versions of the software that would affect the results of this report. FLUENT uses a control-volume-based technique to convert a general scalar transport equation to an algebraic equation that is solved numerically.

Table 2-3. Materials and Properties Used in the Simulations								
	Density		**Specific Heat**		**Thermal Conductivity**		**Viscosity**	
	Kg/m^3	lbm/ft^3	J/kg-K	BTU/lb-°F	W/m-K	Btu/(ft h °F)	Pa-s	$lbf\text{-}s/ft^2$
Lava (Hot)	2,600	162.31	1,100	0.262	1.2	0.69	100	2.1
Lava (Solidified Cooled Substrate)	3,000	187.28	840	0.20	1.2	0.69	—	—
Ground	2,800	174.78	856	0.20	2.25	1.3	—	—

	Latent Heat of Crystallization		**Solidus Temperature**		**Liquidus Temperature**		**Initial Temperature**	
	J/kg	BTU/lb	K	°F	K	°F	K	°F
Lava (Hot)	350,000	150.47	1,273	1831.73	1,473	2191.73	1,500	2,240
Lava (Solidified Cooled Crust)	—	—	—	—	—	—	300	80
Cooled Ground	—	—	—	—	—	—	293	68

It has a pressure-based solver and a density-based solver. While the pressure-based solver is normally used for incompressible flows, the density-based solver is recommended for compressible high Mach number flows. A variety of spatial and temporal discretization schemes, as well as turbulence models, is also available in ANSYS-FLUENT.

For these simulations, the solutions to the full two-dimensional Navier-Stokes equations are obtained using an unsteady, implicit approach. The Semi-Implicit Pressure Linked Equations Consistent (SIMPLEC) algorithm (Van Doormal and Raithby, 1984) is used to treat pressure–velocity coupling for stability. The third-order Monotone Upstream-Centered Schemes for Conservation Laws (MUSCL) (Van Leer, 1979) scheme is used to derive the face values of different variables for the spatial discretization; these variables are used to compute the convective fluxes. The upwind difference scheme is used for its enhanced numerical stability.

The pressure-based solver is used in conjunction with the Green-Gauss, cell-based gradient option. An implicit time-marching scheme is used for faster convergence. Temporal discretization is achieved through a second-order implicit method (second-order backward Euler scheme) (Gresho, et al., 1980). The solutions assumed a Newtonian viscosity for the lava. Non-Newtonian viscosity is not included in the models and the simulations. The solutions are initiated in the unsteady mode. The timestep used for the unsteady simulations varied between 0.01 and 0.1 days. The computations were conducted on a Sun Fire X4100 cluster configured with 10 dual-core AMD Opteron 200 series processors with 16 GB RAM per processor.

3 RESULTS AND DISCUSSIONS

To gain insights into the effects of different temperature-based configurations (with varying degree of cooling histories of the top and bottom lobes) on the cooling of the combined domain and associated thermal fields, current simulations focused on two scenarios consisting of two tabular bodies of lava cooling together with a cooler lobe at the bottom and a hotter lobe at the top. Two different configurations have been considered in these two scenarios. In the first configuration/scenario, the bottom lobe is at 3 months (in terms of cooling under ambient surface conditions and time elapsed after emplacement) while the upper lobe is at 1 month (in terms of cooling under ambient atmospheric conditions) when it is introduced onto the lower lobe. In the second configuration/scenario, the bottom lobe is at 12 months (in terms of cooling under ambient atmospheric conditions) while the upper lobe is 1 month (as described previously). The simulations are carried out with constant viscosity, constant thermal conductivity, and constant density. The influence of rainfall on the exposed lobe top is also considered in the simulations. The value of the convective heat transfer coefficient is taken as 50 W/m^2K [8.8 BTU h^{-1} ft^{-2} $°F^{-1}$] for both configuration simulations. No additional analysis is carried out with variable properties.

3.1 Simulation Results for the First Configuration

Figures 3-1(a–c) through 3-16 show the simulation results for the first configuration, starting where the bottom lobe has been cooling for 3 months and has the top lobe (cooled for 1 month) placed above it. Figure 3-1(a) shows the initial temperature field for the upper and lower lobe as well as the solid, cold substrate. This initial temperature field is constructed from prior simulations carried out with single lobes (Basu, et al., 2012). Figure 3-1(b) and 3-1(c) show an enlarged view of the junction area between the upper and the lower lobe. The gradual change in temperature in this region can be observed from Figures 3-1(b) and 3-1(c). Figures 3-2 through 3-7 shows the simulated temperature fields for very early times (5–60 days) after cooling starts. Once can observe that significant temperature changes take place at the intersection of the upper and lower lobe within the first 60 days. The temperature increases by almost 350 K [630 °F] in the first 60 days. This can be attributed to the cooler top portion of the lower lobe undergoing a temperature increase when it contacts the hotter upper lobe.

Figures 3-8 through 3-16 show the corresponding simulated temperature field for subsequent simulations, starting with 3 months after initiation of cooling until 60 months after cooling. From the results, one can observe that the topmost part of the upper lobe cools down significantly within this period of 3 to 12 months, thus the crustal thickness {as estimated by the position of the 1,273 K [1,832 °F] isotherm} of the top region increases within the first 12 months. The visco-elastic limit is 1,273 K [1,832 °F] even with a 1,500 K [2,240 °F] initial starting temperature. The combined effect of rain and convective cooling from the top surface lowers the temperature of this region. Simultaneously, one can also observe that the temperature in the intersection of the upper and lower lobes also increases considerably within this period (3 to 12 months). This is due to the transfer of heat from the hotter upper lobe to the lower cooler lobe. However, the temperature of the lava substrate and the ground doesn't undergo any significant change {~20–30 K [36–54 °F]}. The temperature of the lava substrate and the ground increases by 20–30 K [36–54 °F] during this period.

Figures 3-12 through 3-16 show the progression of the temperature field at 2, 3, 4, and 5 years, respectively. The gradual thickening of the upper crust of the top lobe can be observed; this thickening is significant up to 3 years {~10 m [32.2 ft]}. However, between 3 and 5 years, the

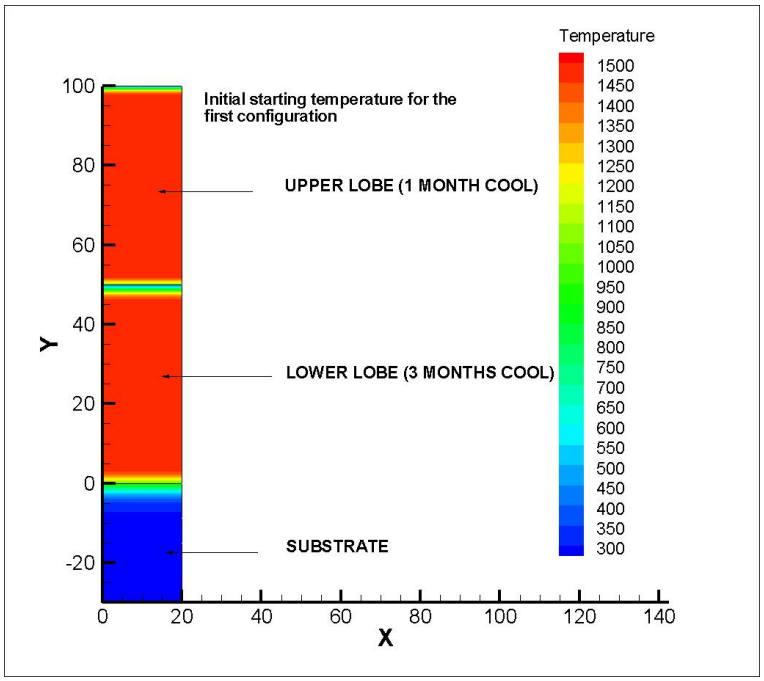

Figure 3-1(a). Initial Temperature Distribution for the First Configuration (Temperature in K)

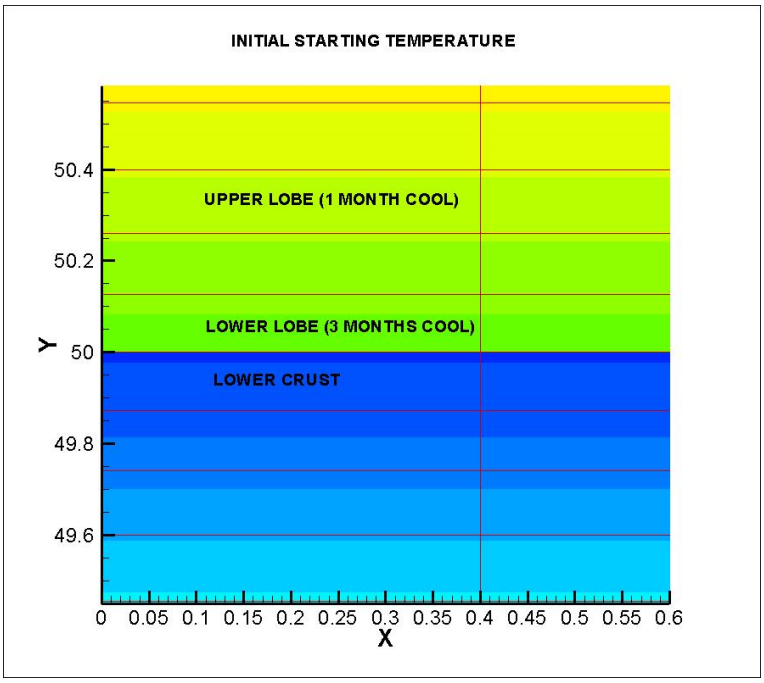

Figure 3-1(b). Initial Temperature Distribution at the Junction Between the Upper and Lower Lobe for the First Configuration (Temperature in K): Grid Lines Are Also Shown for Clarity

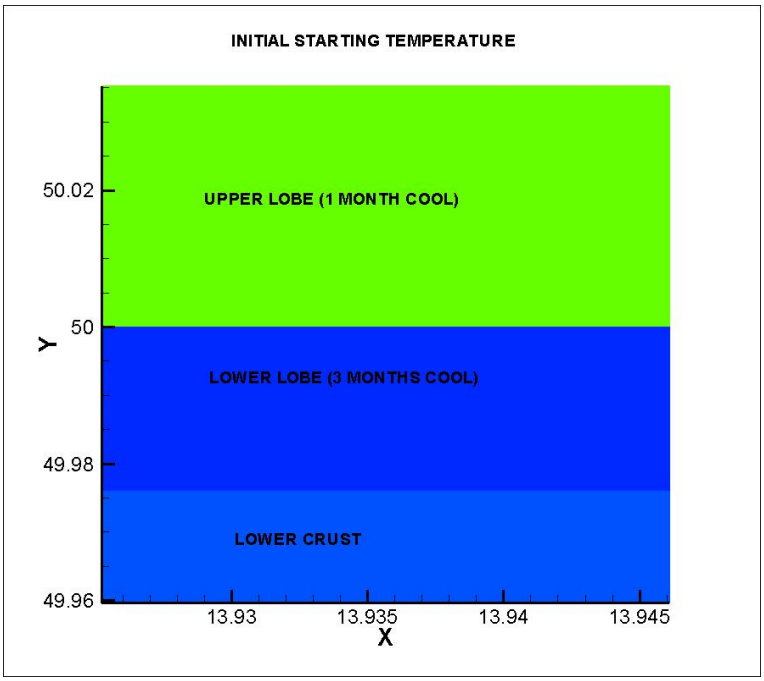

Figure 3-1(c). Initial Temperature Distribution at the Junction Between the Upper and Lower Lobe for the First Configuration (Temperature in K): The Junction Area Is Enlarged

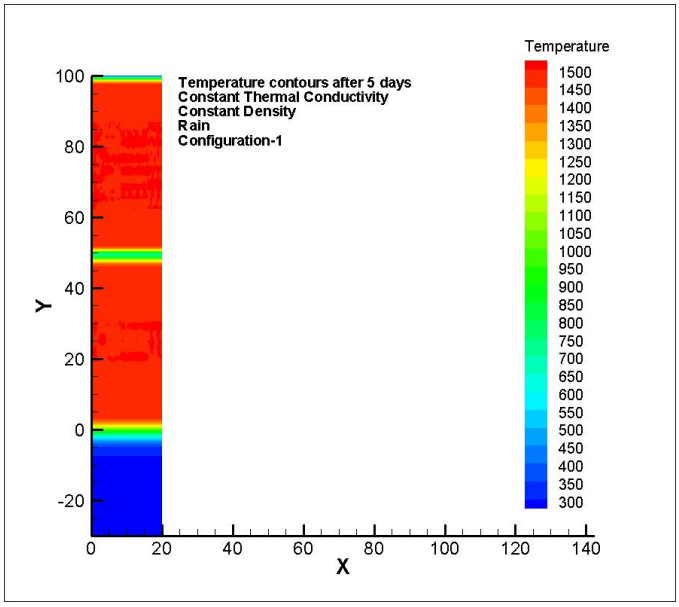

Figure 3-2. Temperature Distribution for the First Configuration After 5 Days

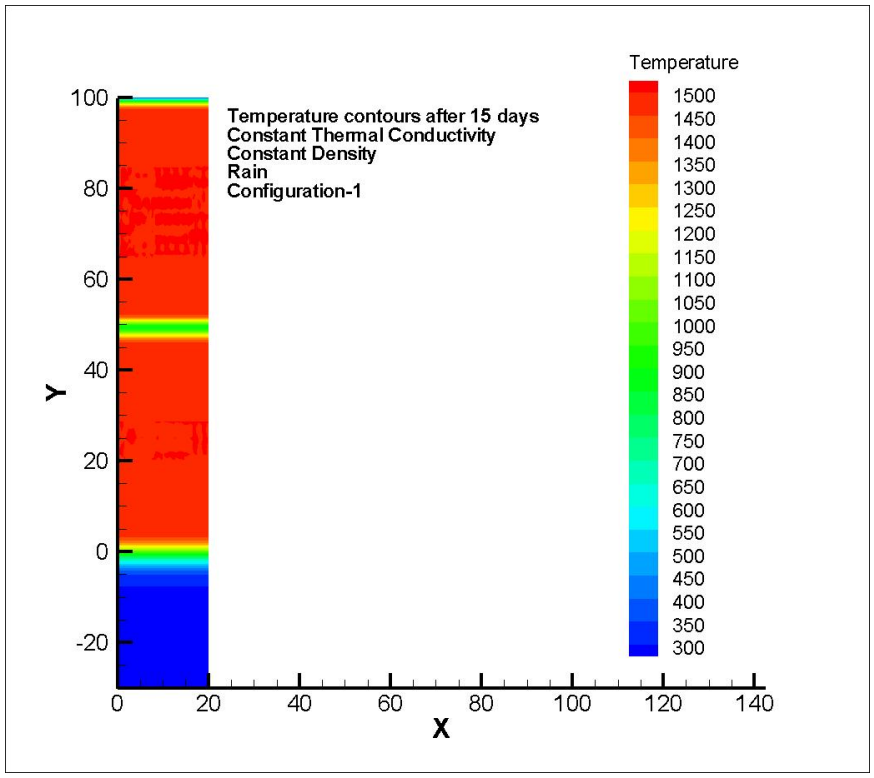

Figure 3-3. Temperature Distribution for the First Configuration After 15 Days

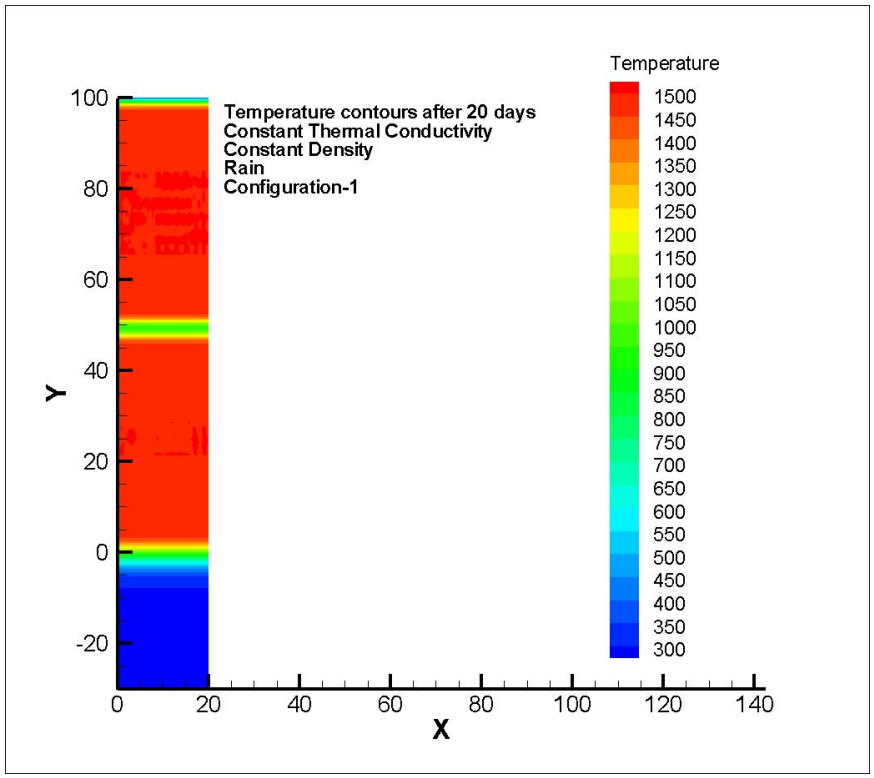

Figure 3-4. Temperature Distribution for the First Configuration After 20 Days

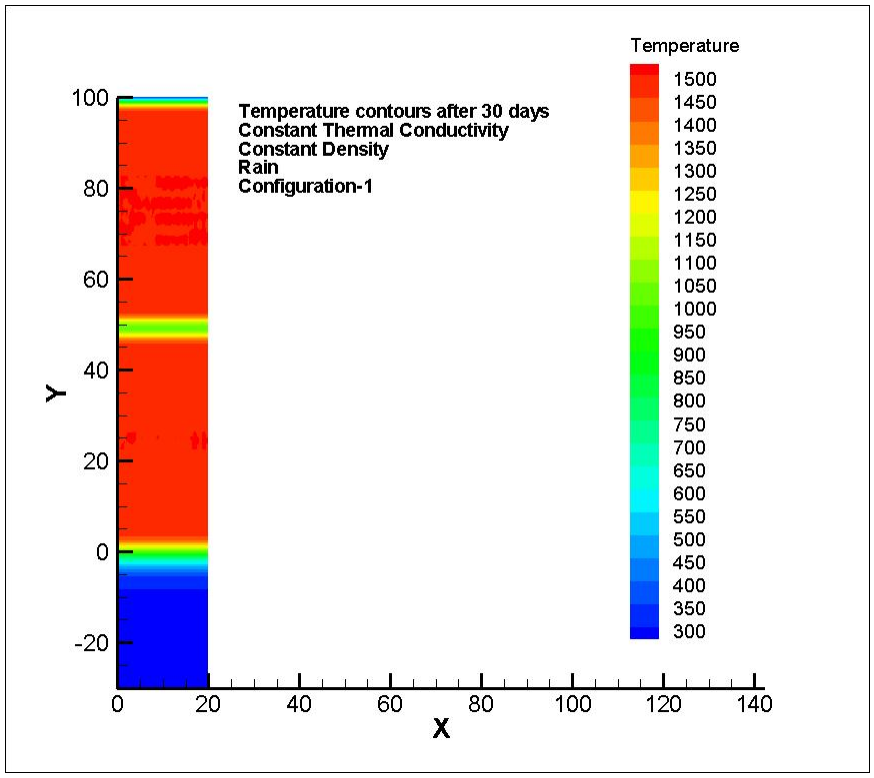

Figure 3-5. Temperature Distribution for the First Configuration After 30 Days

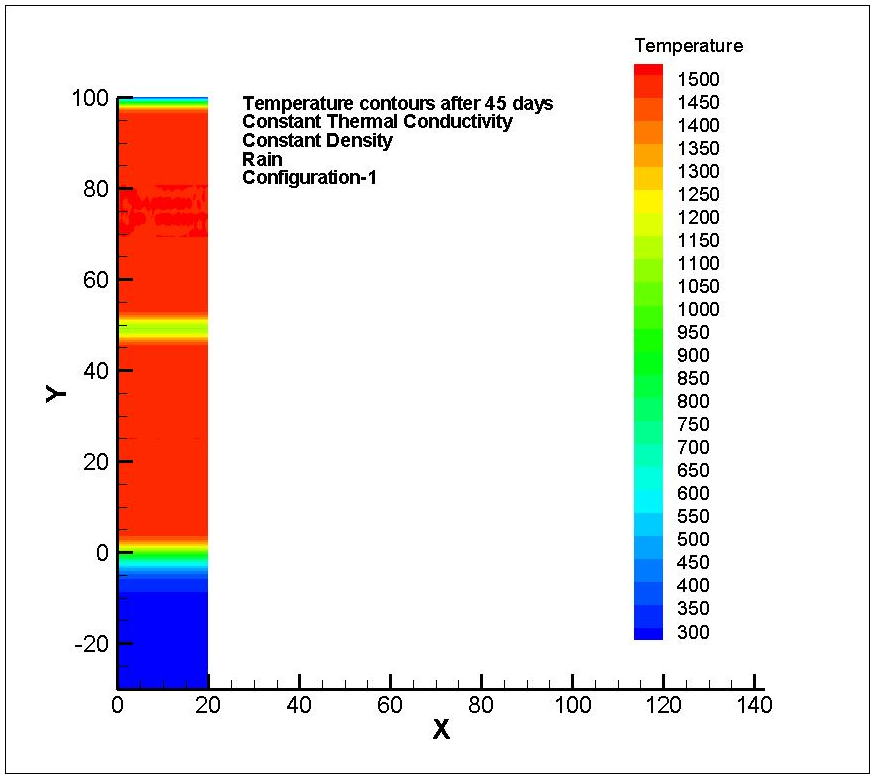

Figure 3-6. Temperature Distribution for the First Configuration After 45 Days

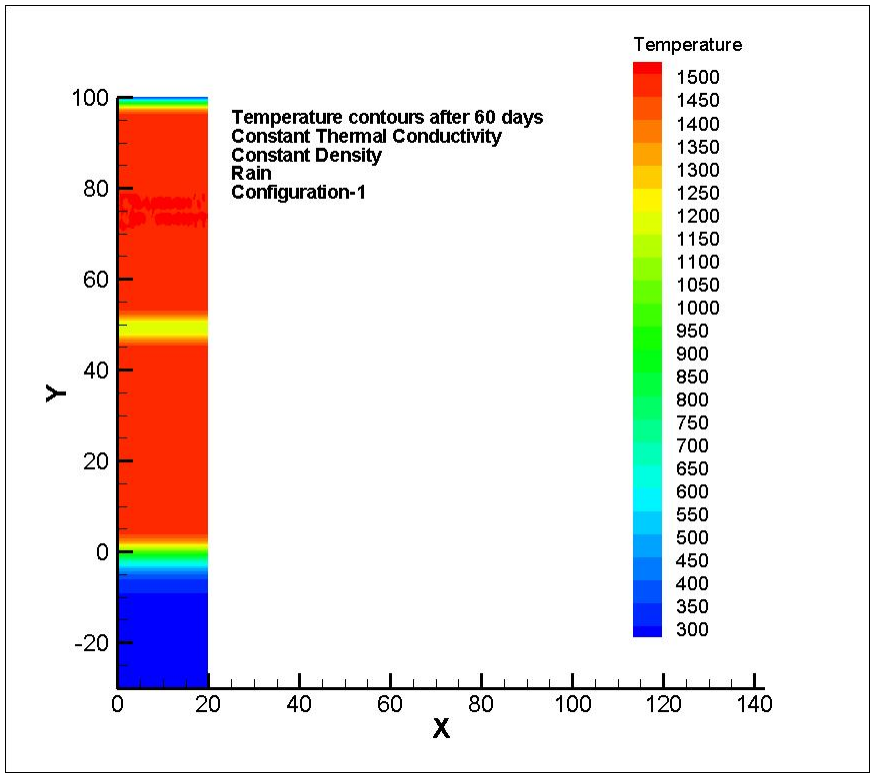

Figure 3-7. Temperature Distribution for the First Configuration After 60 Days

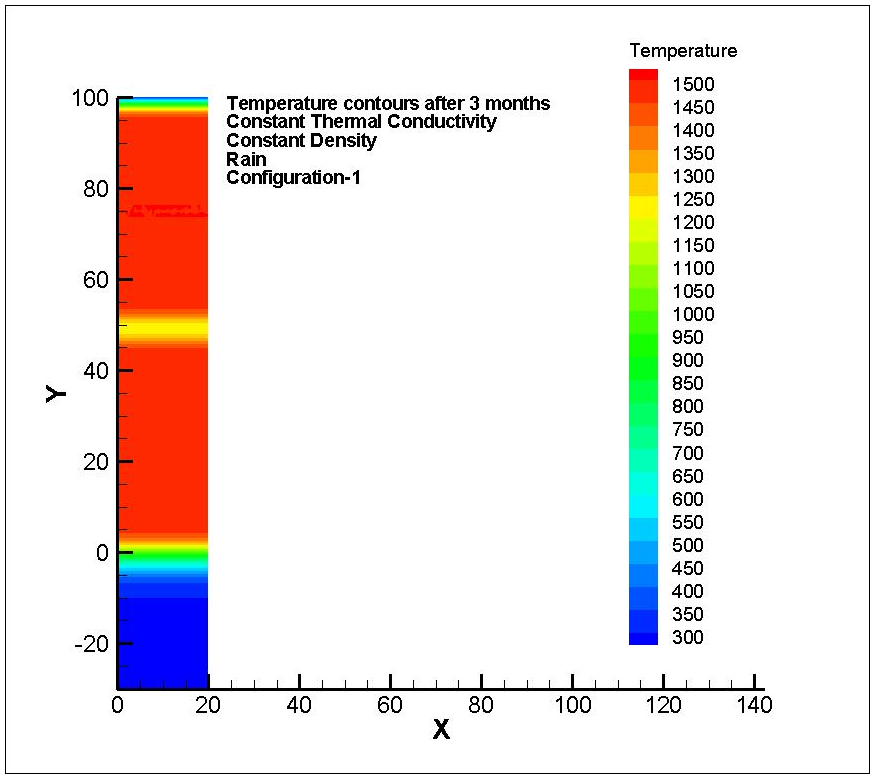

Figure 3-8. Temperature Distribution for the First Configuration After 3 Months

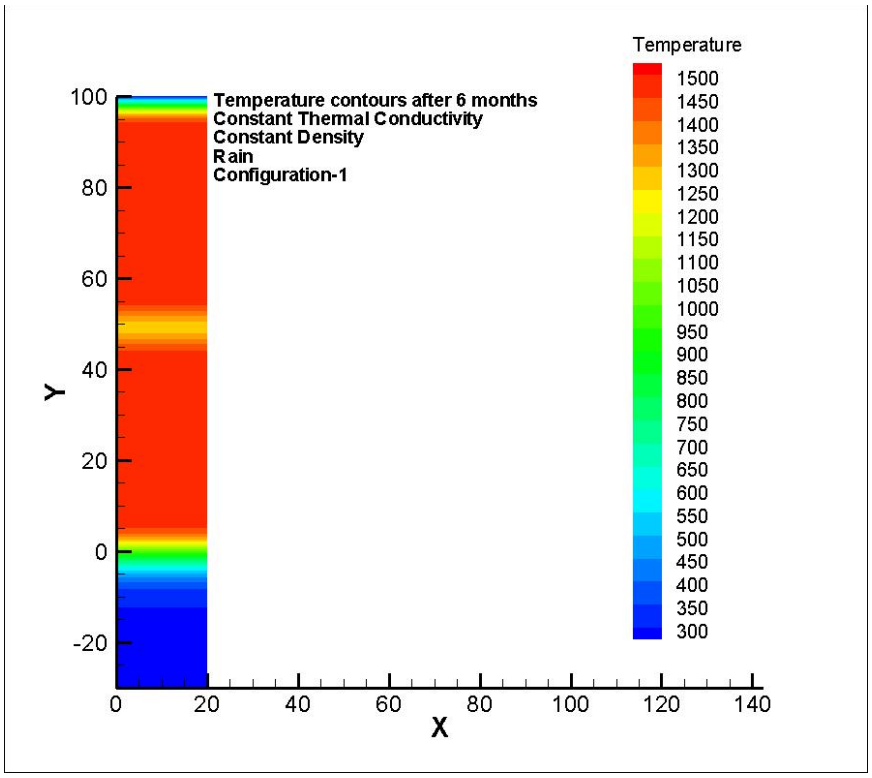

Figure 3-9. Temperature Distribution for the First Configuration After 6 Months

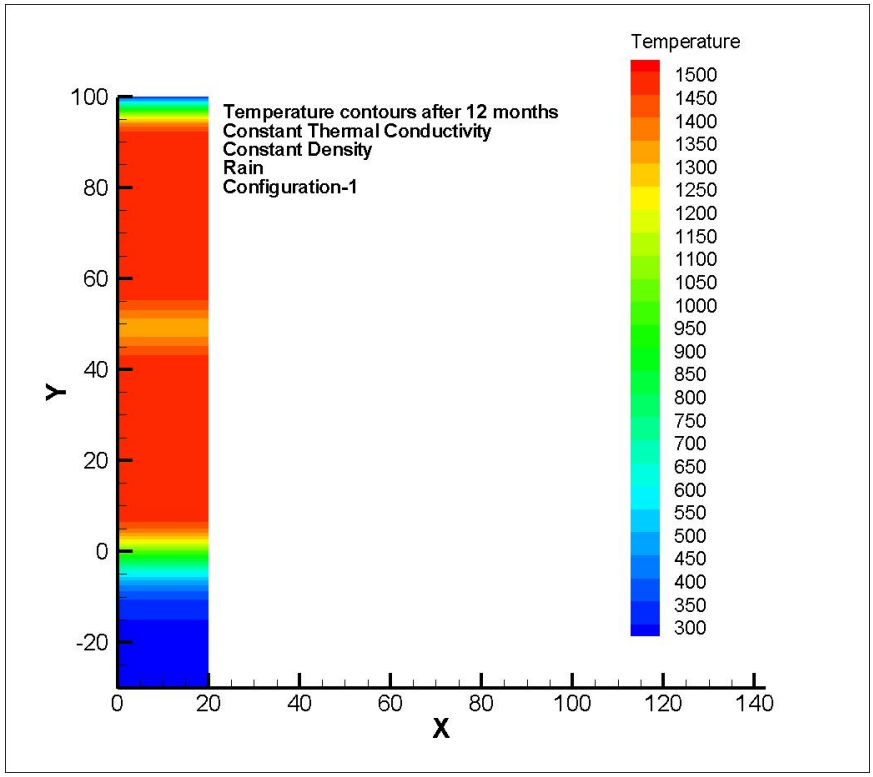

Figure 3-10. Temperature Distribution for the First Configuration After 12 Months

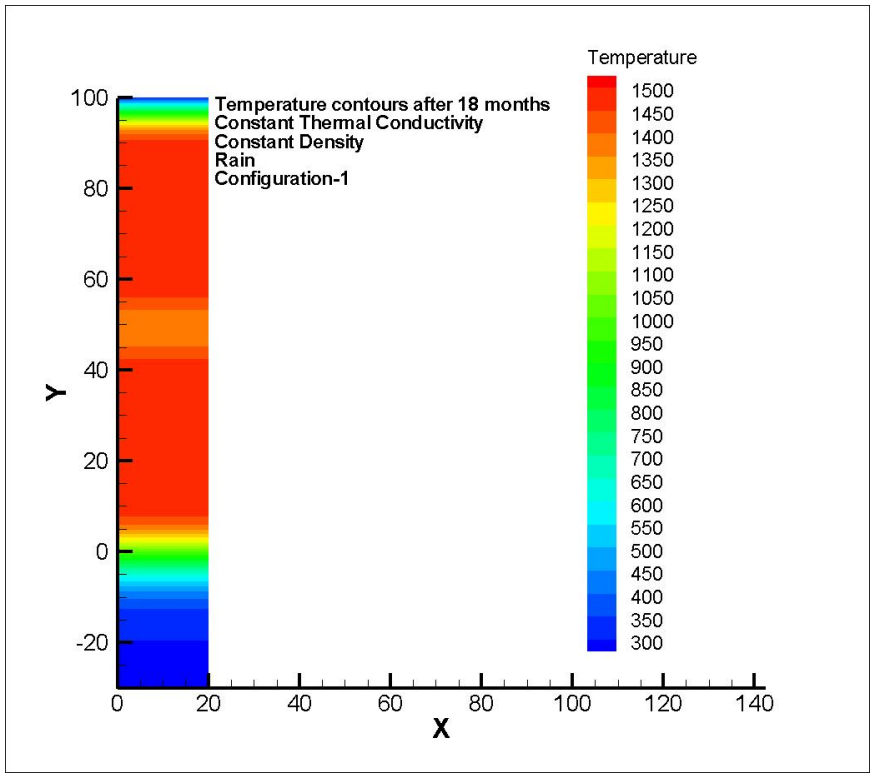

Figure 3-11. Temperature Distribution for the First Configuration After 18 Months

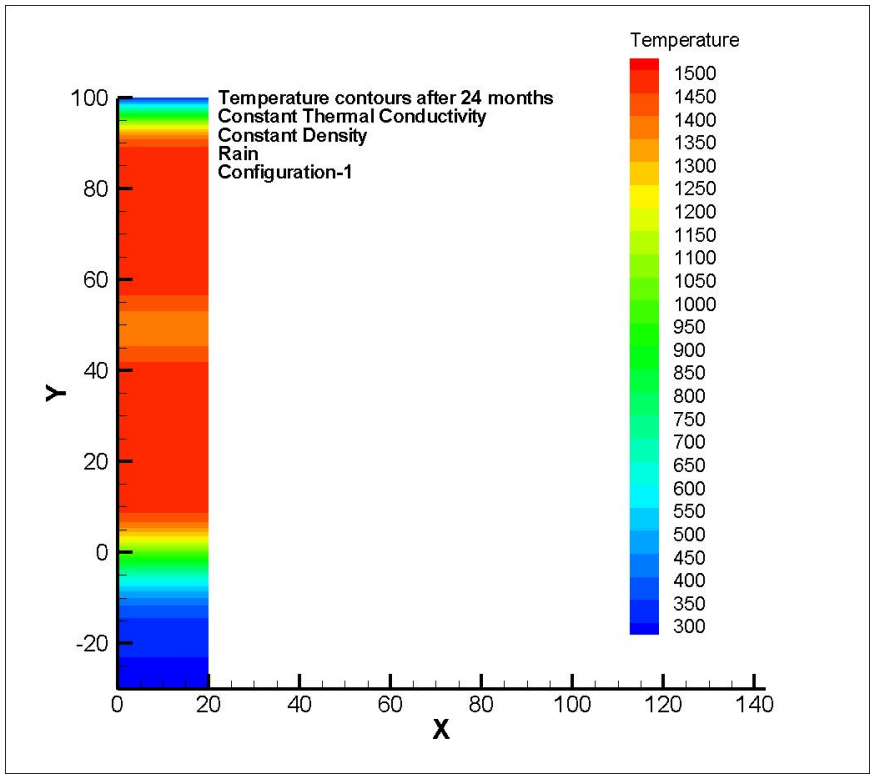

Figure 3-12. Temperature Distribution for the First Configuration After 24 Months

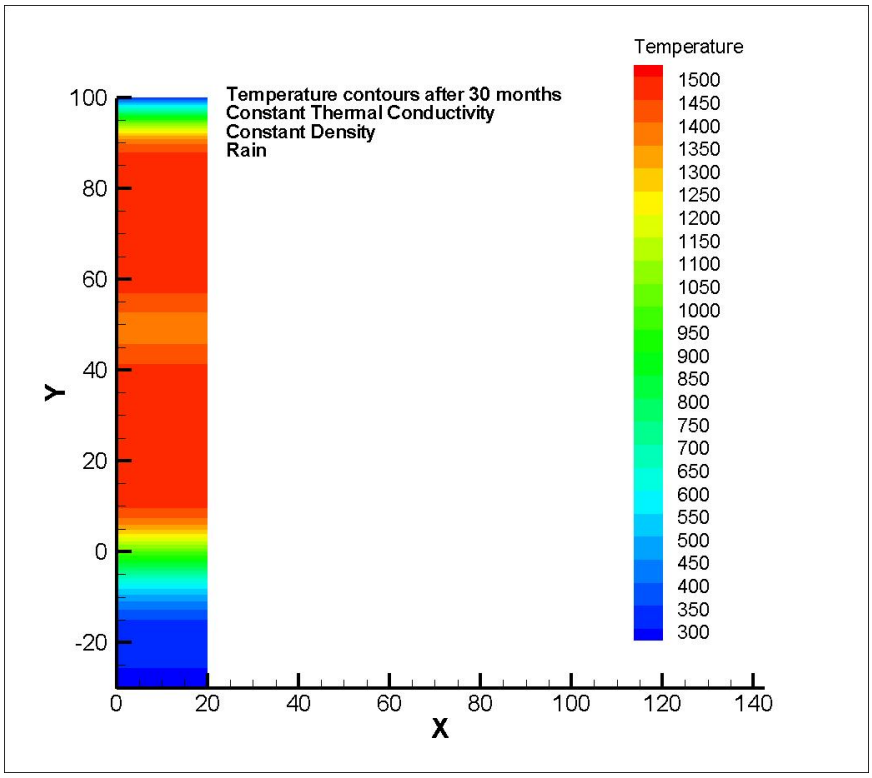

Figure 3-13. Temperature Distribution for the First Configuration After 30 Months

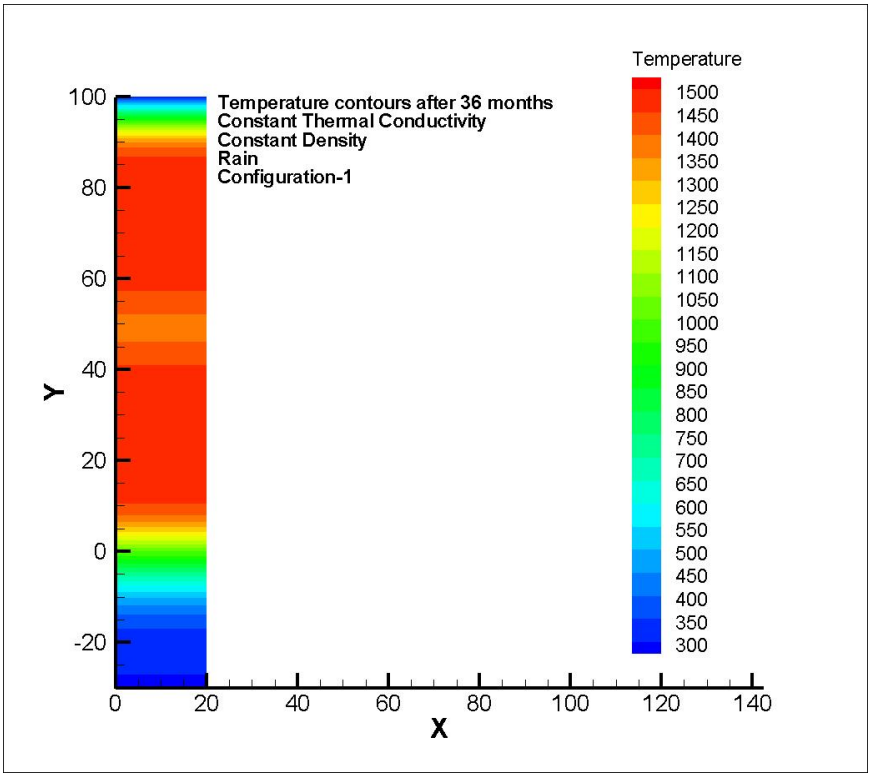

Figure 3-14. Temperature Distribution for the First Configuration After 36 Months

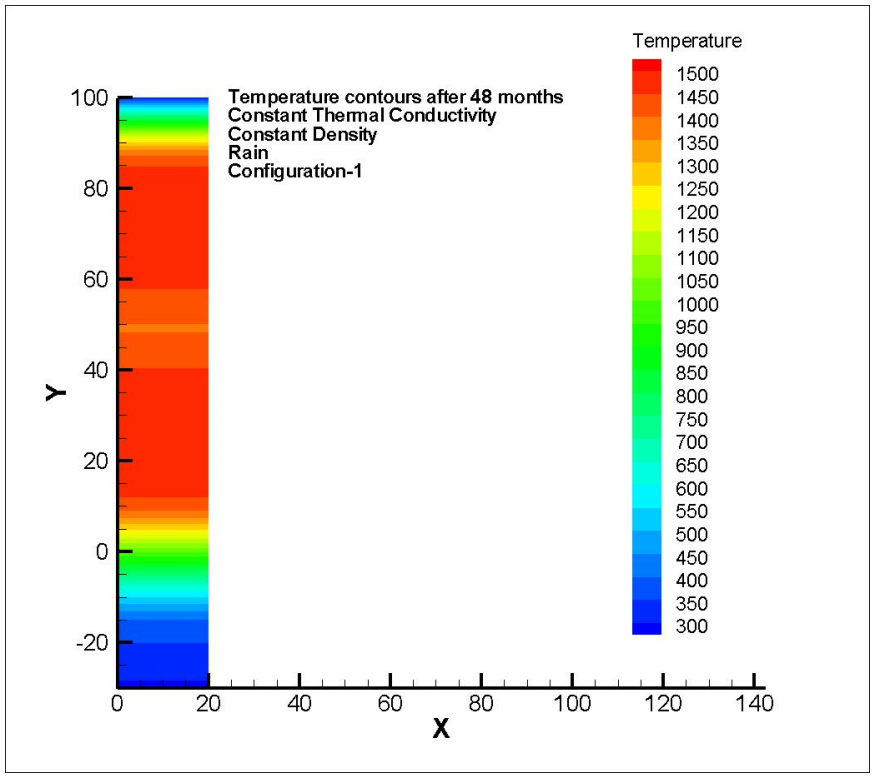

Figure 3-15. Temperature Distribution for the First Configuration After 48 Months

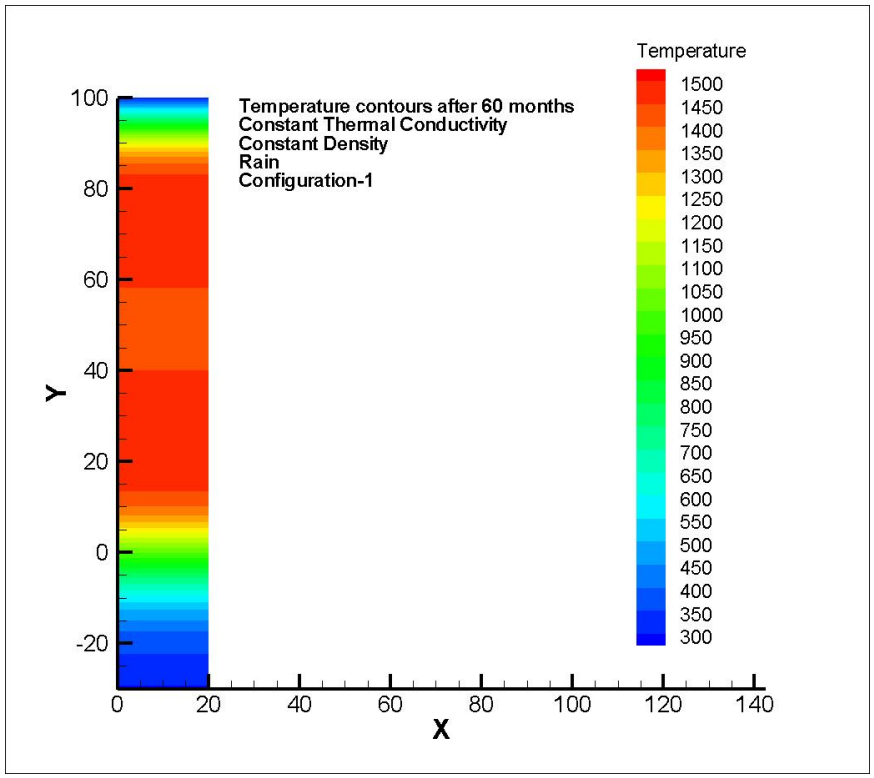

Figure 3-16. Temperature Distribution for the First Configuration After 60 Months

increase in the crustal thickness is only on the order of 2 to 5 m [6.4 to16 ft]. In the first 3 years, the upper crust thickens from rapid cooling caused by rain and convective heat transfer from the upper surface. However, after 3 years, the upward heat transfer from the interface of the two lobes and consequent rise in temperature of the interface of the two lobes slows down both the overall cooling process and the progression of the crustal thickness. Hon, et al. (1994), show crust growth/thickening slows down over time, based on their empirical relationship. In fact, they showed that the change is almost exponential. However, it can be observed that the temperature at the interface region between the top and bottom lobes increases significantly over 5 years. Close observation also reveals that the temperature of the solidified lava substrate and associated ground rocks under the bottom lobe slightly increases in the 5 years. When comparing the present results with that obtained from single-lobe simulations, single-lobe and two-lobe simulations do not appear to differ in terms of temperature penetration into the substrate.

Figures 3-17 through 3-22 show the internal temperature gradient varies with lava cooling as a function of time, which provides insight into the progression of the thermal front with time inside the whole configuration, including the top lobe, the bottom lobe, and the interface region. These temperature profiles at different time intervals were obtained along a vertical line at the mid-section of the computational domain. The values of the temperature obtained along the vertical line are plotted as a function of the depth/height. Figure 3-17 shows the enlarged view of the interface region and the variation of the internal temperature gradient across the region for the first 60 days. It can be observed that there is almost a 700 K [1,260 °F] increase in temperature of the interface region over the first 60 days of cooling. On close observation, one can see that the initial minimum temperature is not at 50 m [164 ft], but somewhat lower at 49.75 m [163.2 ft]. In addition, the minimum temperature shown in this plot is around 430 K [315 °F], which is higher than 300 K [80 °F] (the initial temperature of the intersection). This discrepancy can be attributed to numerical errors and mesh quality. The current level of computational grid used in these simulations is unable to capture the exact temperature change in the interface region. A very fine grid clustered near the intersection would have been able to predict exactly 300 K [80 °F] at 50 m [164 ft] (interface between top and bottom lobes). Figure 3-18 shows the temperature variation across the interface region over 5 years. It shows the enlarged view of the interface region and the variation of the internal temperature gradient across the region. This can be observed from Figure 3-1(b) and 3-1(c) as well. As mentioned previously, it can be observed that temperature in the interface region increases from 450 K (initially) to 1,150 K [350 to 1,610 °F] in the first 60 days of cooling, an increase of almost 700 K [1,260 °F]. However, between 60 days and 5 years, the temperature increases by only 300 K [540 °F] for the interface region. It can also be observed that the relative increase in temperature slows down significantly between 3 and 5 years. This is probably because the interface region reaches a thermal equilibrium with the top and the bottom lobes after 3 years, and hence the temperature change becomes much less prominent between 3 and 5 years. In addition, one can also see the movement of the lava temperature minimum into the upper crust of the bottom lobe by a 1–2 meters (3.28–6.6 ft). The slopes are also slightly different above and below the minimum. This is expected, because the top and the bottom lobe have different cooling times for the initial conditions of the two lobes.

Figure 3-19 shows the enlarged view of the solidified lava substrate and ground (solid lava) region below the bottom lobe and the variation of the internal temperature gradient across the region. Here the initial temperature at the start of the simulations is the result of 3 months of heating of the substrate by the bottom lobe, shown by the curve labeled *initial temperature*. It can be observed that the temperature increase in this region close to the ground and

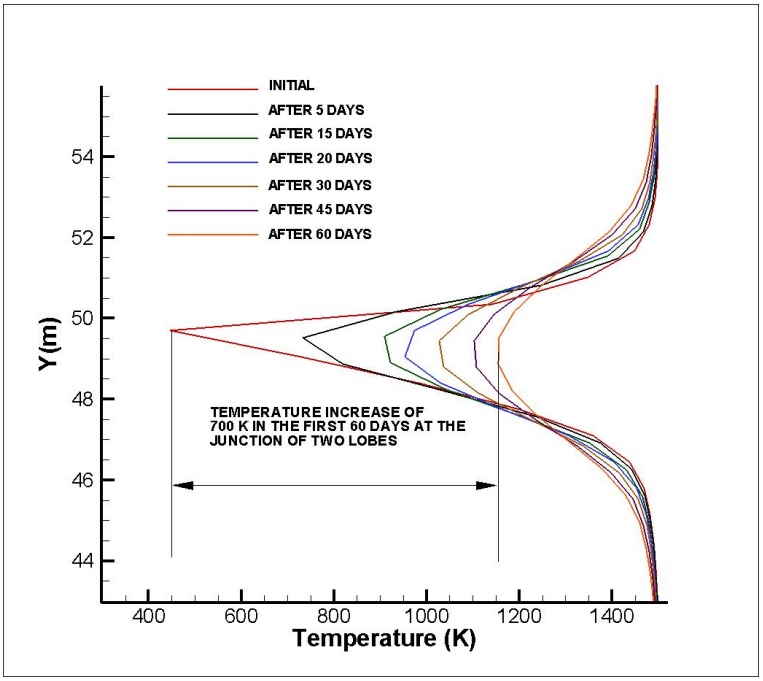

Figure 3-17. Variation of Internal Temperature Gradient Over the First 60 Days of Cooling: Temperature Distribution Close to the Intersection Zone (Contact) (Approximately @ 49.75) of the Two Lobes for the First Configuration

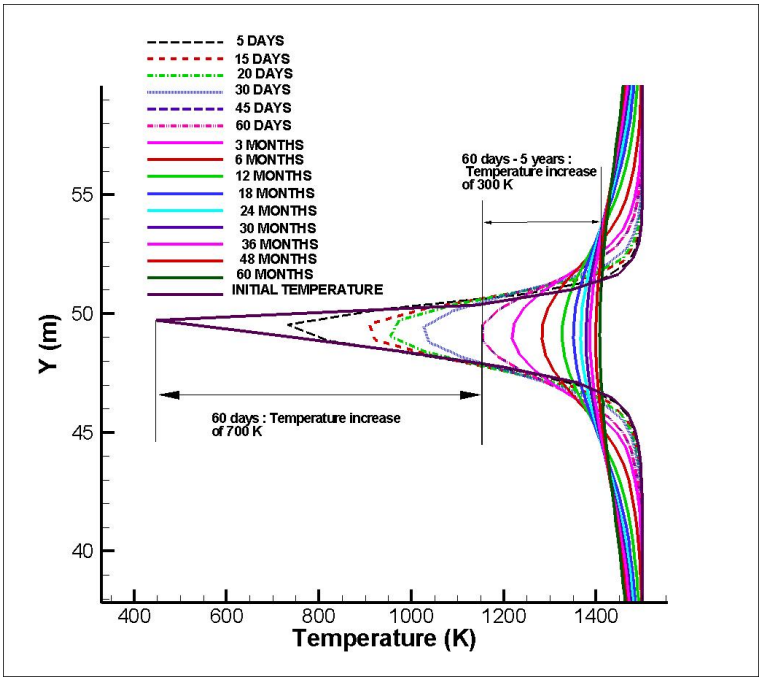

Figure 3-18. Variation of Internal Temperature Gradient Over 5 Years of Cooling: Temperature Distribution in the Intersection Region Between the Upper and Lower Lobe for the First Configuration

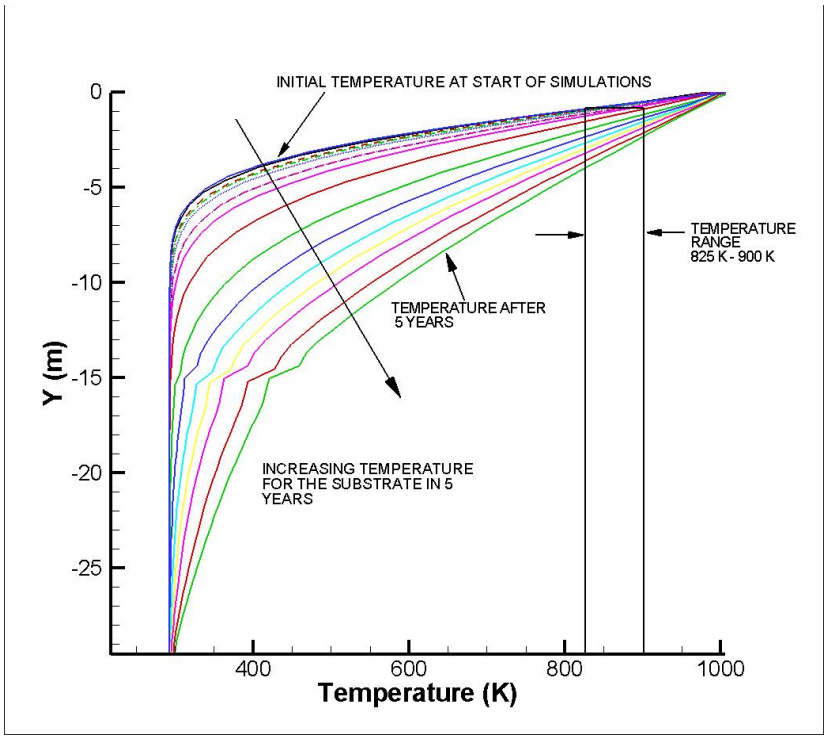

Figure 3-19. Variation of Internal Temperature Gradient Over 5 Years of Cooling Under the Lower Lobe: Temperature Distribution in Substrate for the First Configuration

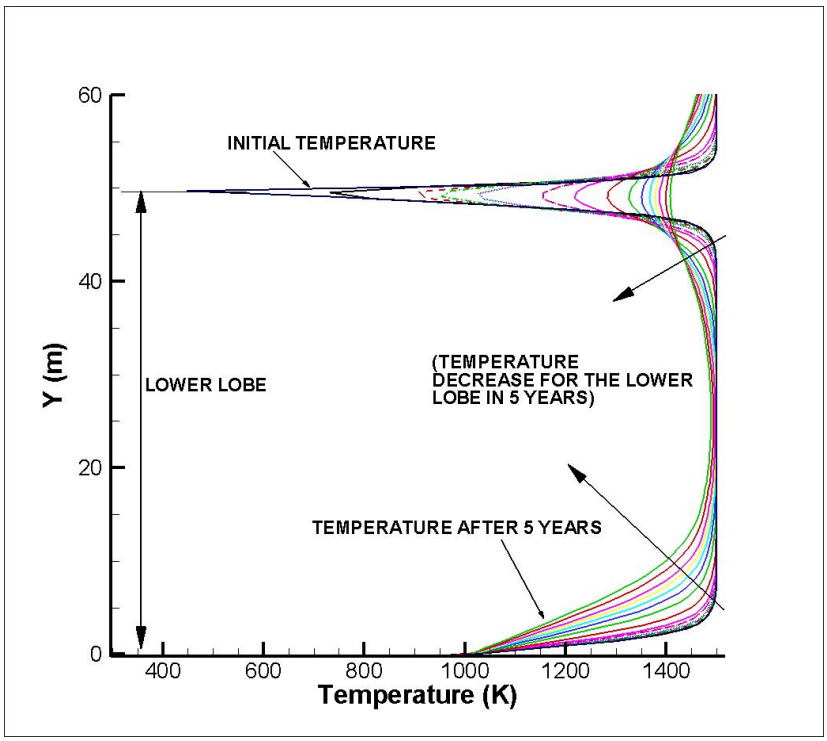

Figure 3-20. Variation of Internal Temperature Gradient Over 5 Years of Cooling: Temperature Distribution in the Lower Lobe for the First Configuration

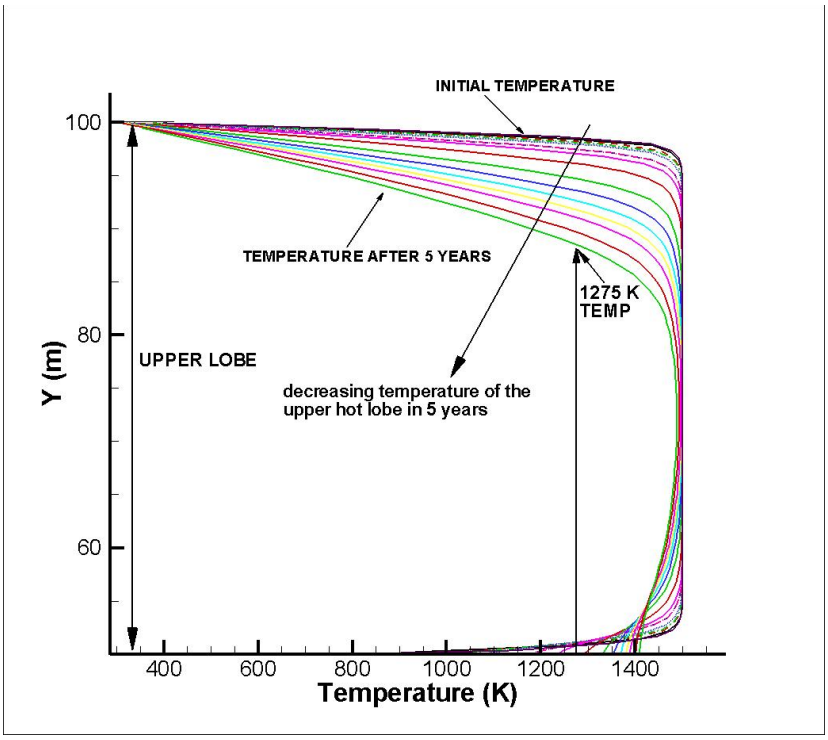

Figure 3-21. Variation of Internal Temperature Gradient Over 5 Years of Cooling: Temperature Distribution in the Upper Lobe, Which Started at 1 Month of Cooling

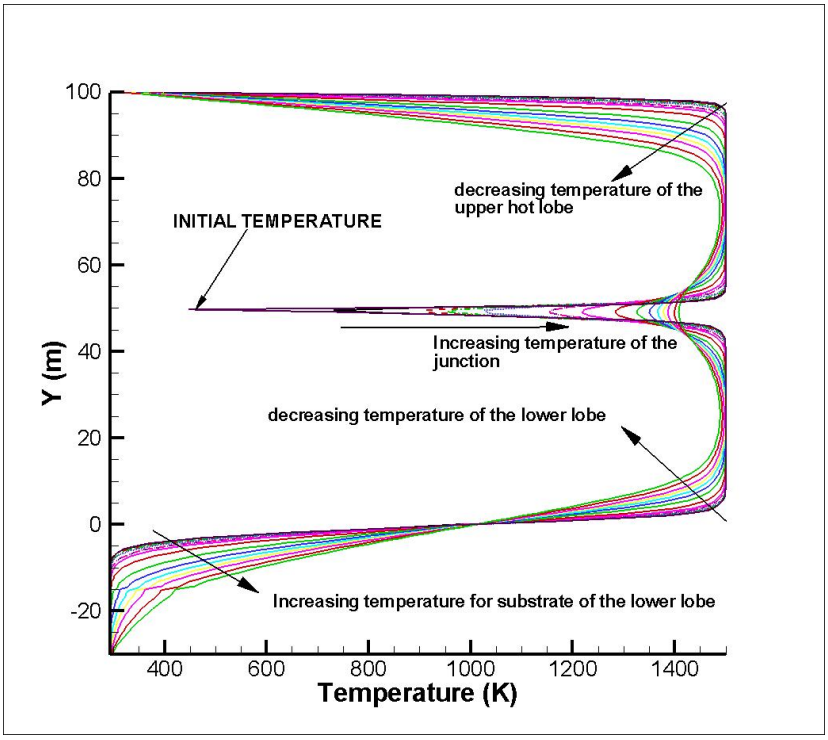

Figure 3-22. Variation of Internal Temperature Gradient Over 5 Years of Cooling: Temperature Distribution Over the Whole Region

substrate ranges from approximately 250 to 450 K [450 to 810 °F] over the 5-year period. At 10 m [32.8 ft], the temperature increase is around 300 K [540 °F]. Near the contact with the substrate, temperatures rise from cold/ambient to 800–900 K [980–1,160 °F] over 5 years. This is almost all a product of heating by the lower lobe. This 400–600 K [720–1,080 °F] rise is seen at a few meters' depth in the substrate. This is expected because the heat flux from the interface region is conducted down to the region below the lobe and consequently the substrate is heated for a prolonged period. On close observation in Figure 3-19, one can see that there is a kink at 15 m [38 ft], which is a manifestation of the change in rock properties in the initial set up. This clearly shows that the numerical scheme is able to reflect the change in rock properties between the substrate and lower crust of the lower lobe. A rectangular bar has been added in the figure showing the temperature range of 825–900 K [1,025–1,160 °F]. This is the range for Curie temperature for the magnetic materials in basalts. This shows that shows that the top 5 m [16 ft] or so would be heated above the Curie temp and its magnetic minerals would be reset by re-heating.

Figure 3-20 shows the enlarged view of the lower lobe and the temperature variation across the lower lobe over 5 years. The temperature of the lower lobe decreases by almost 200 K [360 °F] over the 5 year period over a height of 8 m [26 ft] above the base of the lower lobe. While the temperature of the solidified lava substrate and ground increases with time, the temperature of the lower lobe decreases with time and reaches a thermal equilibrium with the solidified lava substrate.

Figure 3-21 shows the temperature variation for the upper lobe in a similar enlarged view of the top lobe and the variation of the internal temperature gradient across the upper crust and the entire top lobe region. While recording the development of the upper crust of the lava lobe, an almost 300 K [540 °F] temperature reduction can be observed for this region because of the cooling of the upper surface from the rain and the convective heat transfer, recording the development of the upper crust of the lava lobe. The temperature drop of 300 K [540 °F] was observed at a 12-m [39.37-ft] depth from the top. At the top, the temperature drop is much lower over the same time and this cooling is independent of the presence of a second lobe beneath it. A significant observation that can be made from Figure 3-21 is that the temperature at which the basalt crust stops growing is 1,275–1,300 K [1,835–1,880 °F]. The temperature is attained at 12 m [39 ft] in 5 years. This is exactly the same observation Hon, et al. (1994) made for cooling of a single lobe, with modification by Keszthelyi (2012). This clearly shows that the present computation results are consistent with observations in natural analog sites. Figure 3-22 shows the temperature variation across various zones over the 5 year period.

Based on the simulations, the following conclusions can be made for this lobe configuration. Maximum heating of the top of the lower lobe in the mid-section occurs within the first 3 years. Temperature change in the mid-section interface region slows down after 3 years and further change between 3–5 years is not significant. Below the bottom lobe, the lava substrate (solidified lava overlying limestone) is heated above the starting temperature by 250 to 450 K [450 to 810 °F] over the 5-year period. At 10 m [32.8 ft], the temperature increase is around 300 K [540 °F]. This temperature change of 250 to 450 K [450 to 810 °F] takes place over a depth of 15 m [49 ft] from the bottom of the lower lobe, and the temperature change gradient is almost constant over the years. Basu, et al. (2012) obtained similar results for the lower crust and substrate for a single-lobe configuration. The upper crust of the top lobe develops by cooling over approximately 300 K [540 °F] in 5 years. The temperature change gradient is almost constant over the years.

3.2 Simulation Results for the Second Configuration

Figures 3-23 through 3-44 show the simulation results for the second configuration, where the top lobe has cooled for 1 month before emplacement onto the bottom lobe, which has cooled for 12 months before the top lobe arrives. This initial temperature field is constructed from prior simulations carried out with single lobes (Basu, et al., 2012). Consequently, compared to the first configuration, this second configuration has a lower initial temperature as shown in Figure 3-23. Figures 3-24 through 3-29 show the temperature distribution at different times within the first 60 days of cooling. Compared to Figures 3-2 through 3-7 (for the first configuration), one can clearly observe that the temperature in the interface region is significantly lower for the second configuration {~900 K [1,160 °F]} compared to the first configuration {~1,150 K [1,610 °F]}. This is expected because the top of the bottom lobe in this second configuration has an initial temperature that is lower than that in the first configuration.

Figures 3-31 through 3-38 show the progression of the temperature field for the second configuration at 6 months, 1 year, 18 months, 2 years, 30 months, 3 years, 4 years and 5 years, respectively. It can be clearly observed that over time, the temperature of the upper crust of the top lobe decreases, while the temperature at the interface between the top and bottom lobe increases. The thickness of the upper crust of the top lobe increases as well. The temperature of the bottom lobe, especially the solid lava substrate and the temperature of the adjacent ground, also increases with time. However, the temperature at the interface for this second configuration is significantly lower compared to the temperature at the interface for the first configuration. This is because, in the second configuration, the lower lava lobe has a lower initial upper-surface temperature at the beginning of the simulations. Two important observations can be made from Figures 3-36 through 3-38. First of all, this cooling of the upper lobe for the second configuration is independent of the two-lobe scheme; earlier work by Basu, et al. (2012) also found that there is a similar trend in the temperature gradients for the single lobe case. Second, the results for the 12-month cooling case are almost similar to the results for the 3-month cooling case. This is because the cooling of the lobe top is independent of the presence of the lower lobe, except at the joint/contact region.

One can also observe that the temperature increases in the interface region between the top and the bottom lobe; however, the peak temperature in the interface region is lower for this second configuration compared to the peak temperature in the interface region for the first configuration, as expected. Similarly, one can observe that the crustal thickness at the top of the upper lobe increases, but the rate of increase slows down after 3 years. This is similar to what was observed for the first configuration and can be attributed to the whole configuration reaching thermal equilibrium after 3 years.

Figure 3-39 shows the variation of the internal temperature gradient of the second configuration over the first 60 days of cooling. One can observe a temperature increase of 550 K [990 °F] in the interface region over these 60 days of cooling. To facilitate the understanding of the temperature changes at the interface of the upper and lower lobes, an enlarged view of the temperature profiles at the interface region is shown in Figure 3-40. From Figures 3-39 and 3-40, one can observe that the initial temperature of the interface region was around 400 K [260 °F], and subsequently, the temperature at the interface region increases to around 1,320 K [1,916 °F] in 3 years. Initially, this temperature at the interface was controlled by the top surface temperature of the lower lobe {300 K [80.33 °F]} and the bottom surface temperature of the upper lobe {1,000 K [1,340 °F]}. Hence, there is a temperature increase of 900 K [1,620 °F] in the first 3 years. This is because a small zone heats up quickly. However, between 3 and 5 years, the temperature increases from 1,320 to 1,380 K [1,916 to 2,024 °F]—a comparatively

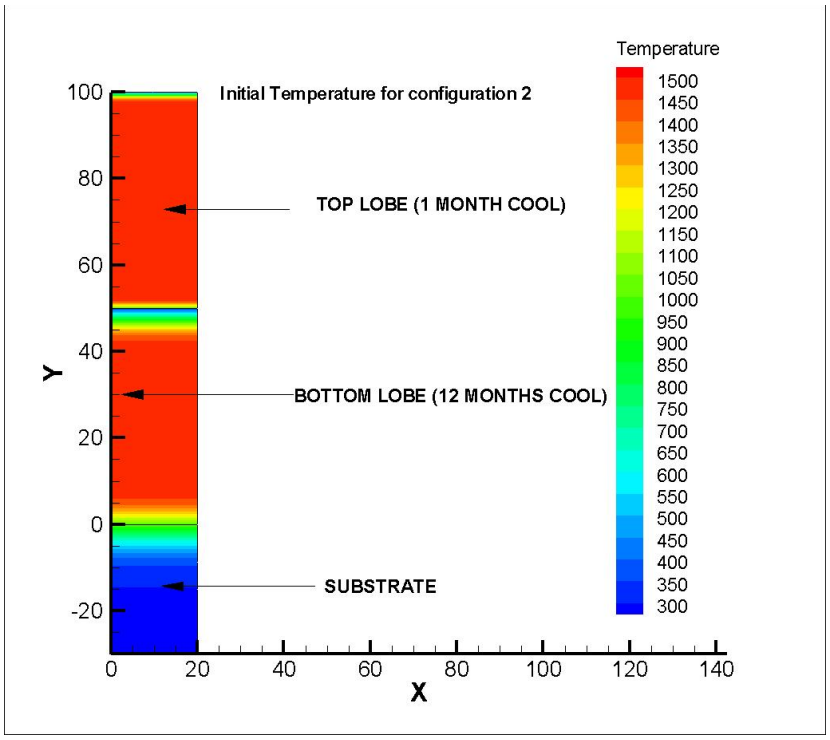

Figure 3-23. Initial Temperature Distribution for the Second Configuration, Which Involves a 1-Month Cooled Top Lobe and a 12-Month Cooled Bottom Lobe

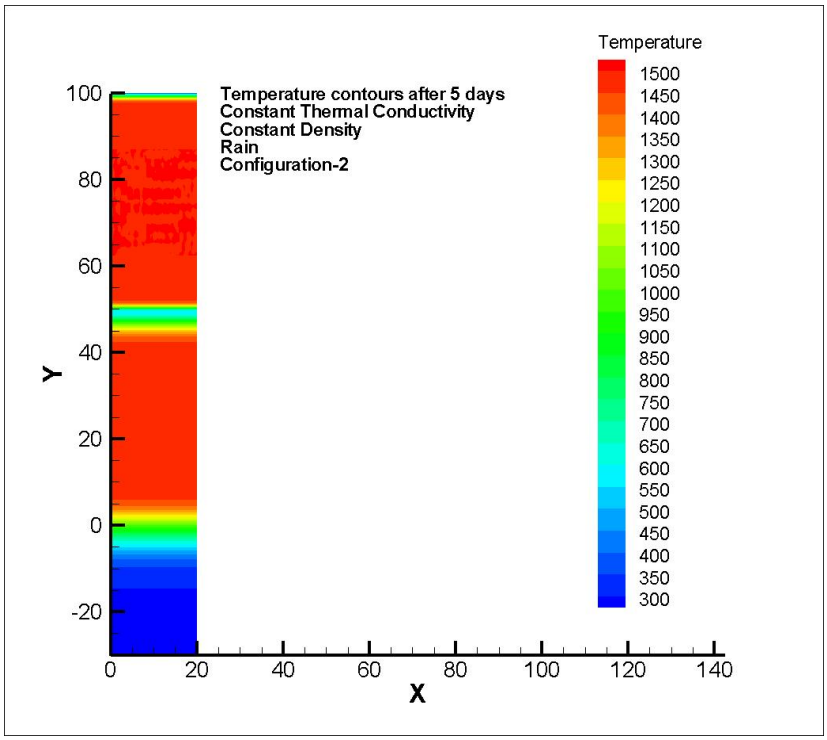

Figure 3-24. Temperature Distribution for the Second Configuration After 5 Days

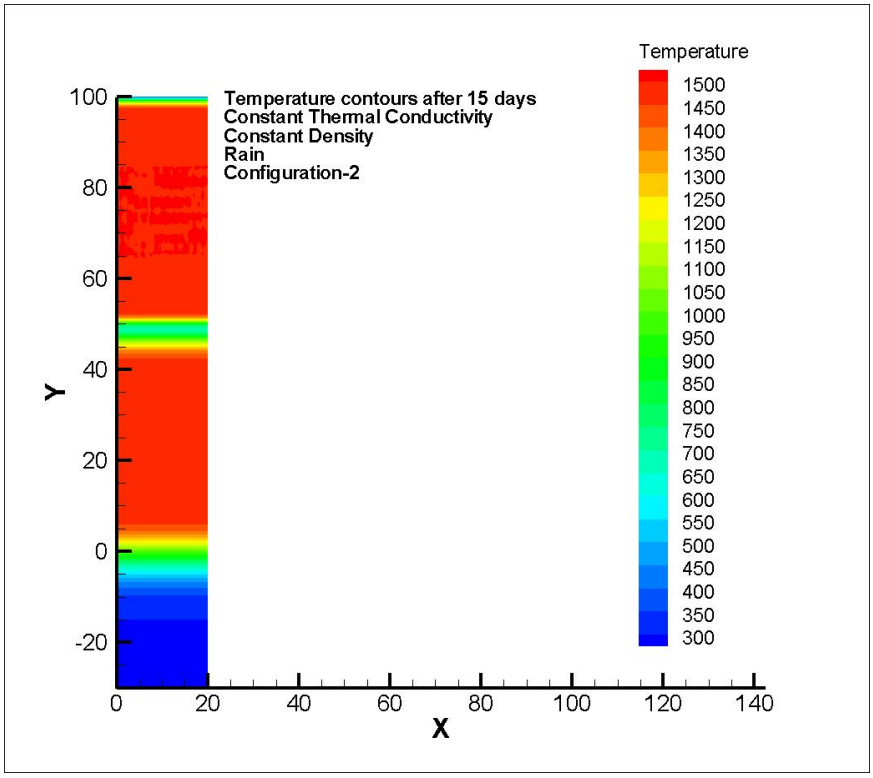

Figure 3-25. Temperature Distribution for the Second Configuration After 15 Days

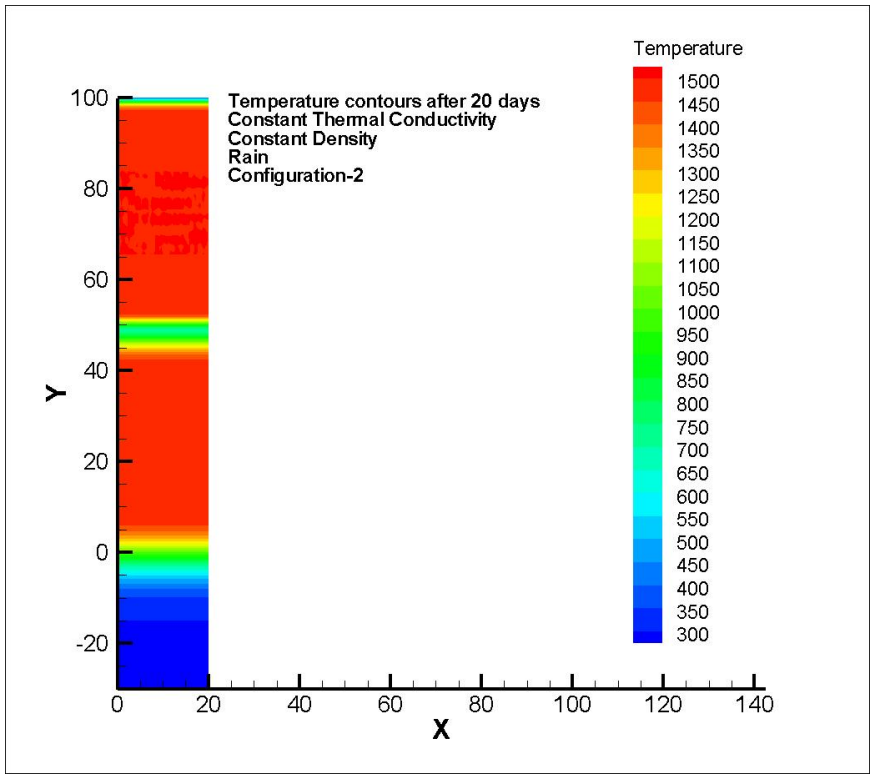

Figure 3-26. Temperature Distribution for the Second Configuration After 20 Days

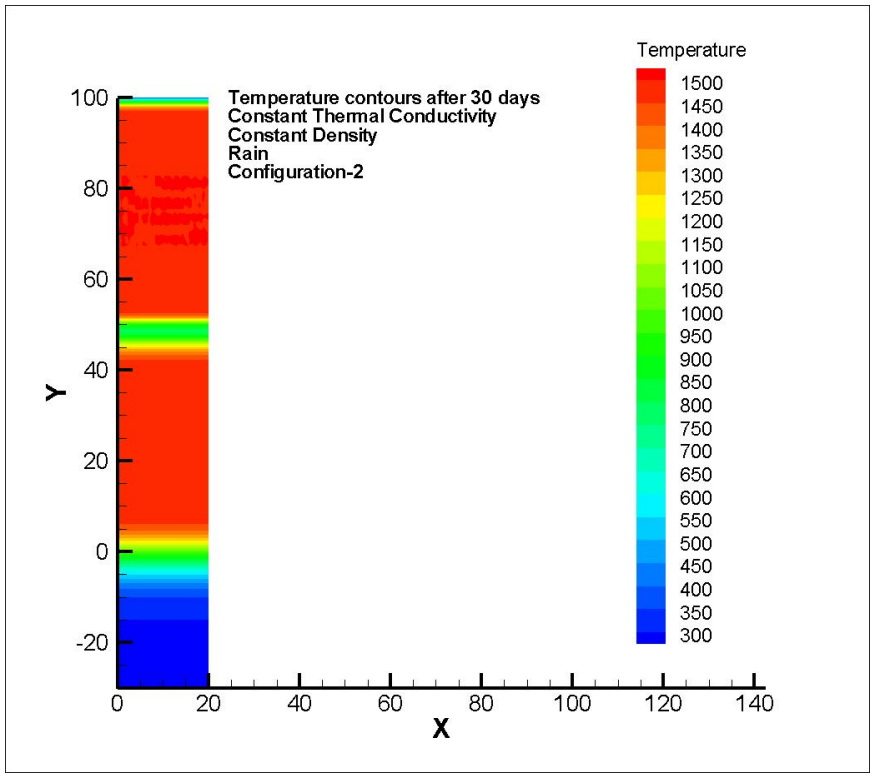

Figure 3-27. Temperature Distribution for the Second Configuration After 30 Days

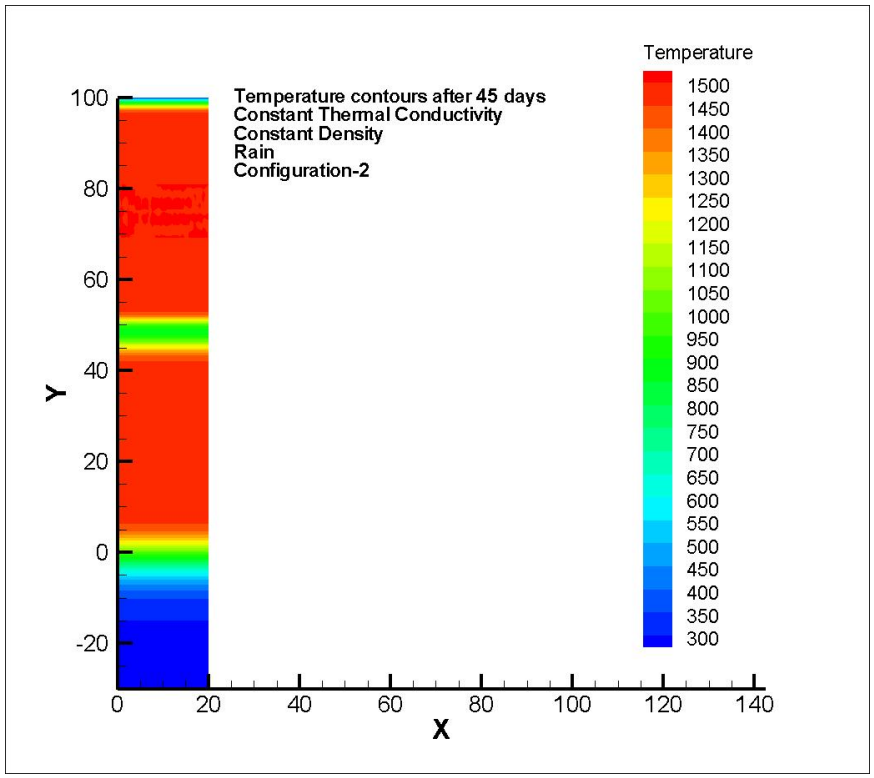

Figure 3-28. Temperature Distribution for the Second Configuration After 45 Days

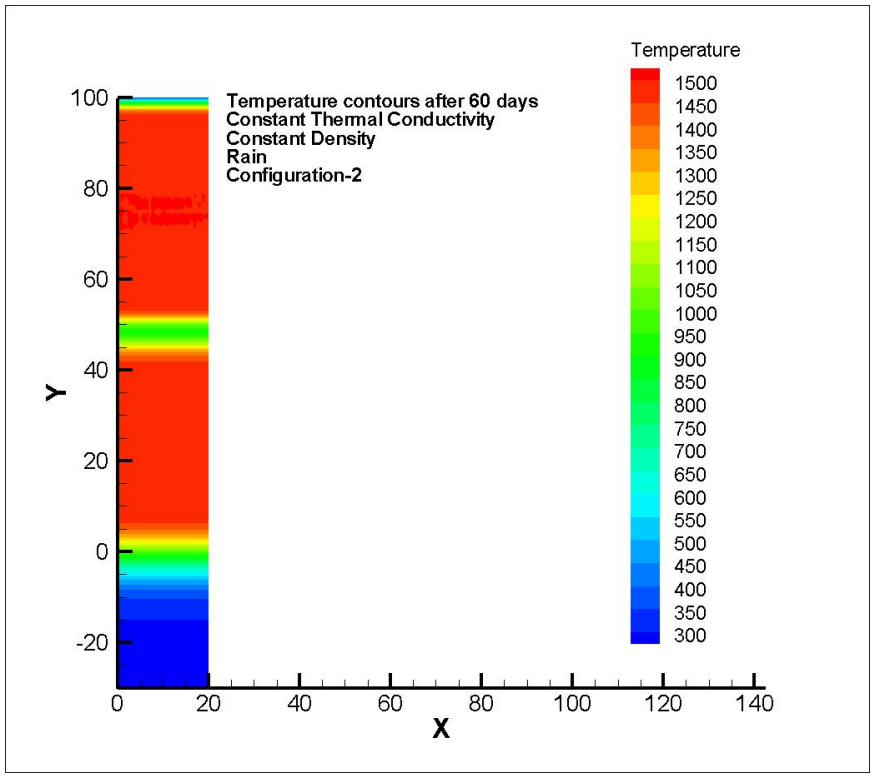

Figure 3-29. Temperature Distribution for the Second Configuration After 60 Days

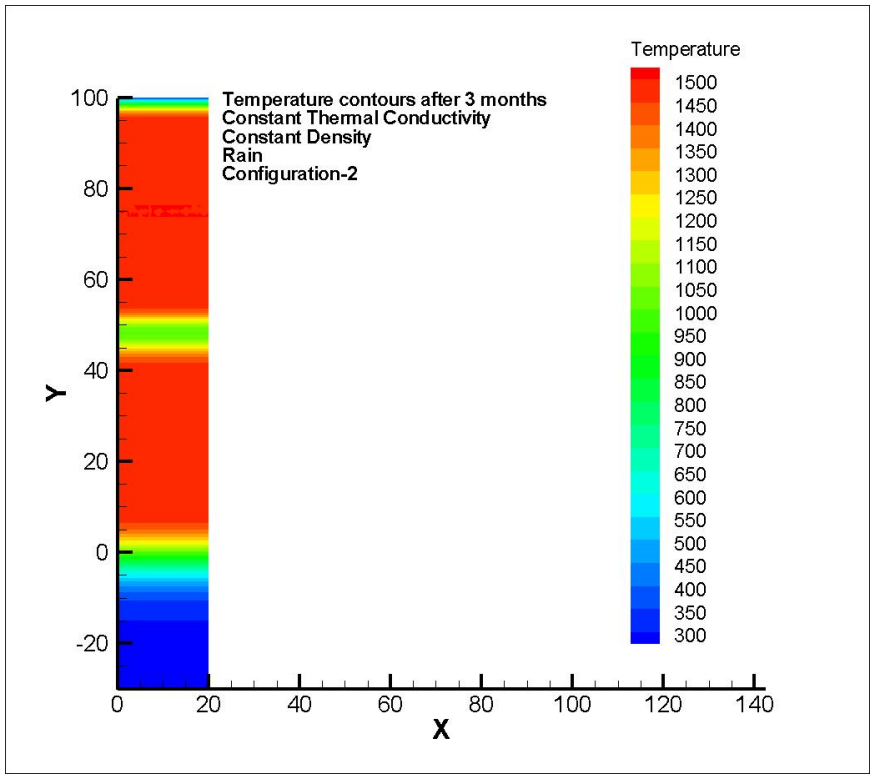

Figure 3-30. Temperature Distribution for the Second Configuration After 3 Months

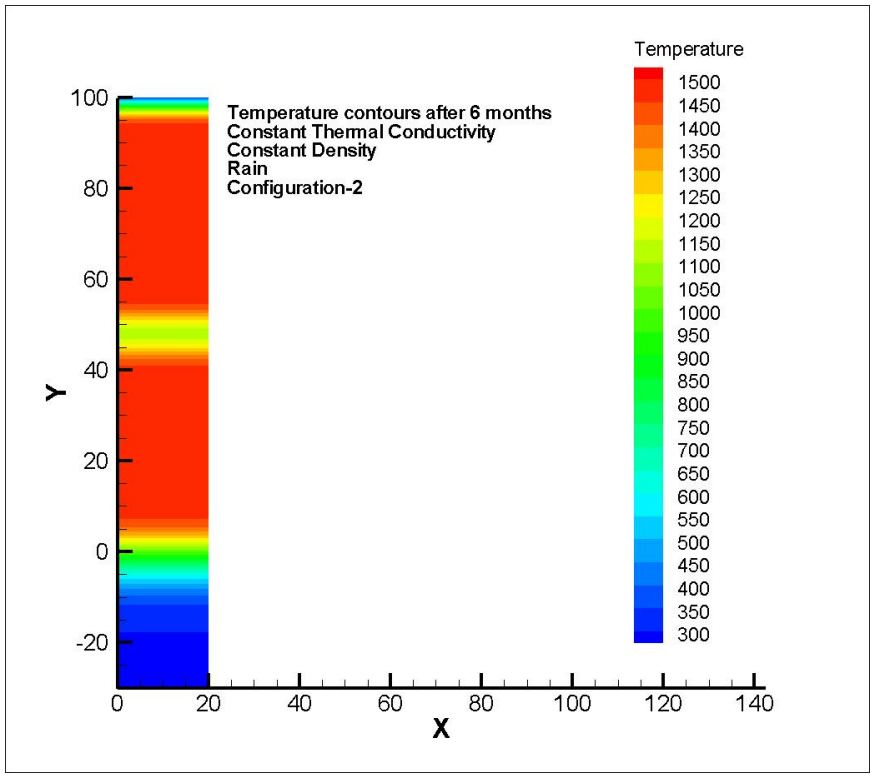

Figure 3-31. Temperature Distribution for the Second Configuration After 6 Months

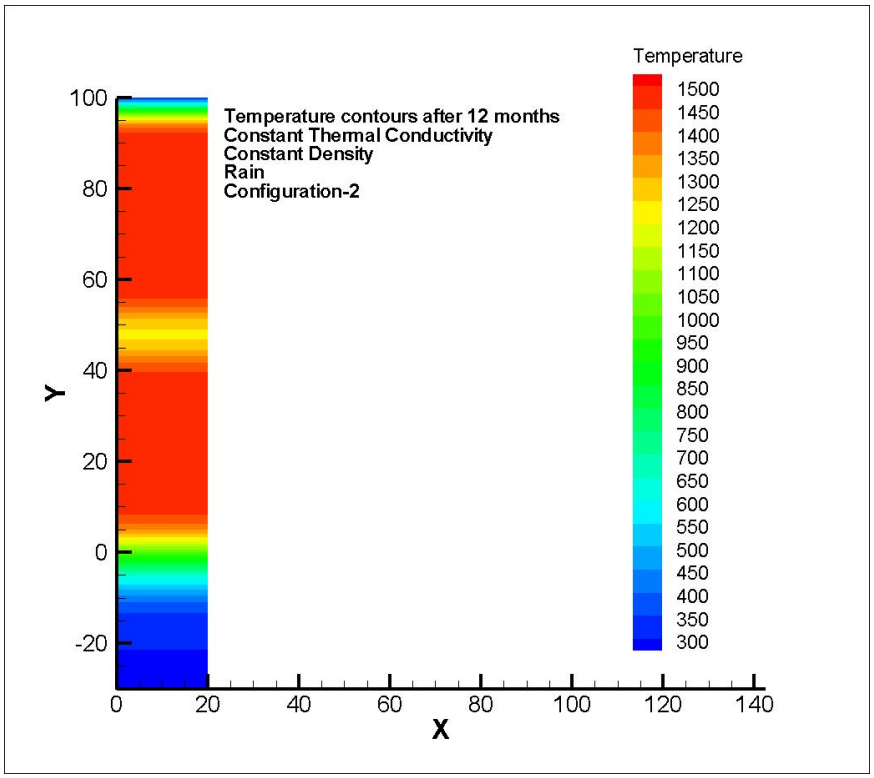

Figure 3-32. Temperature Distribution for the Second Configuration After 12 Months

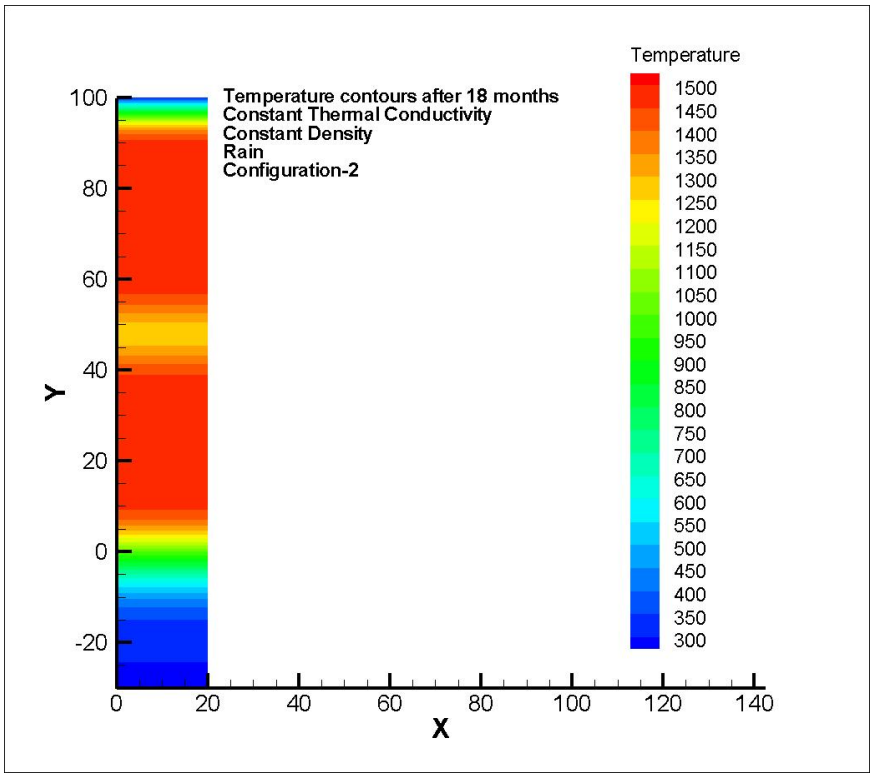

Figure 3-33. Temperature Distribution for the Second Configuration After 18 Months

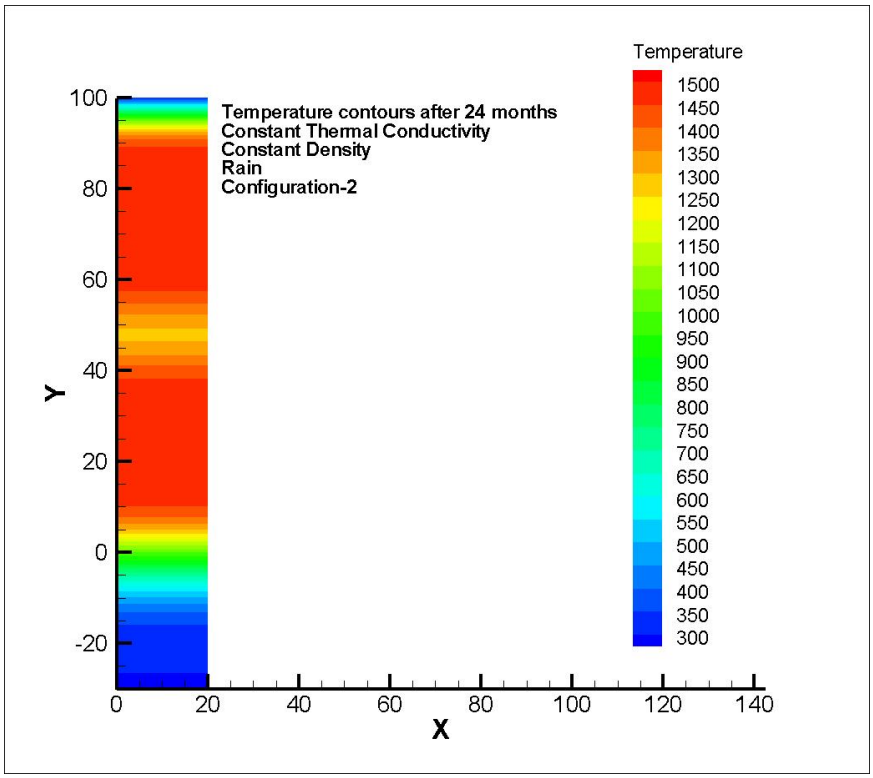

Figure 3-34. Temperature Distribution for the Second Configuration After 24 Months

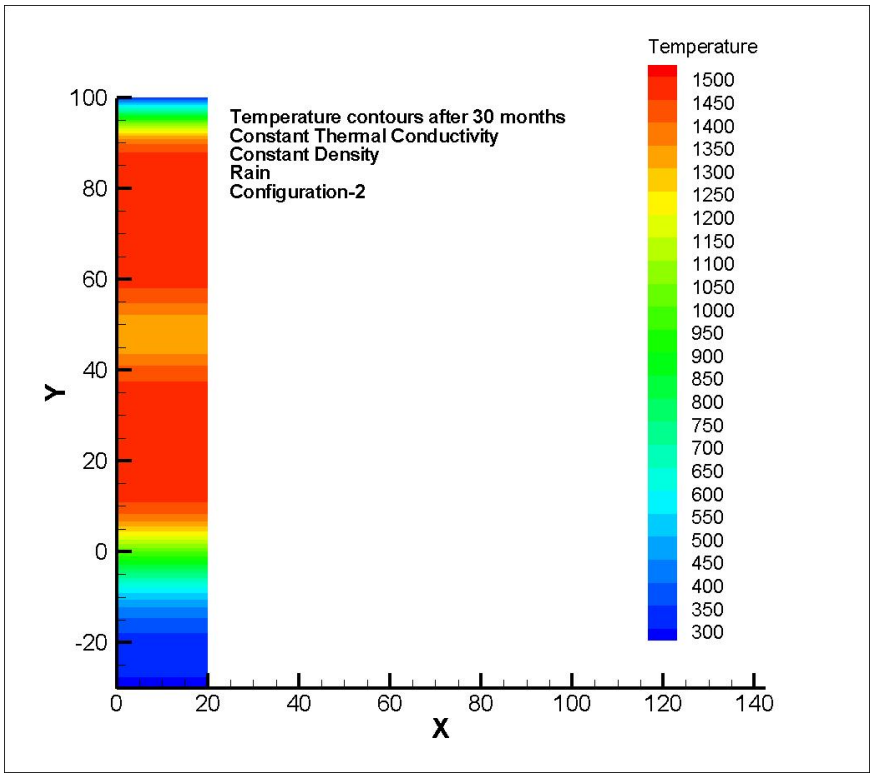

Figure 3-35. Temperature Distribution for the Second Configuration After 30 Months

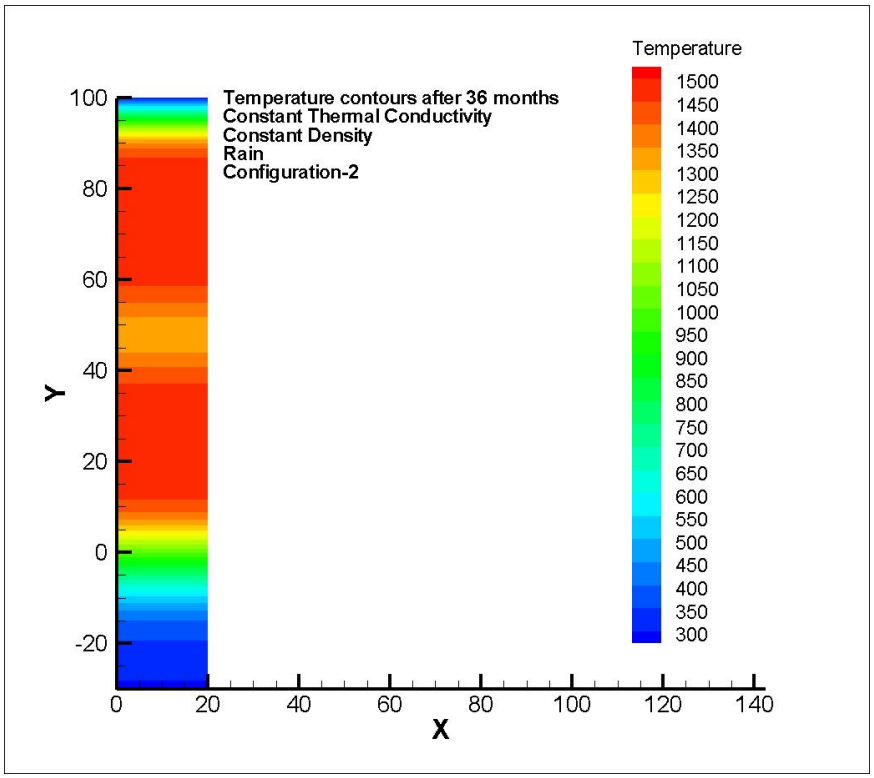

Figure 3-36. Temperature Distribution for the Second Configuration After 36 Months

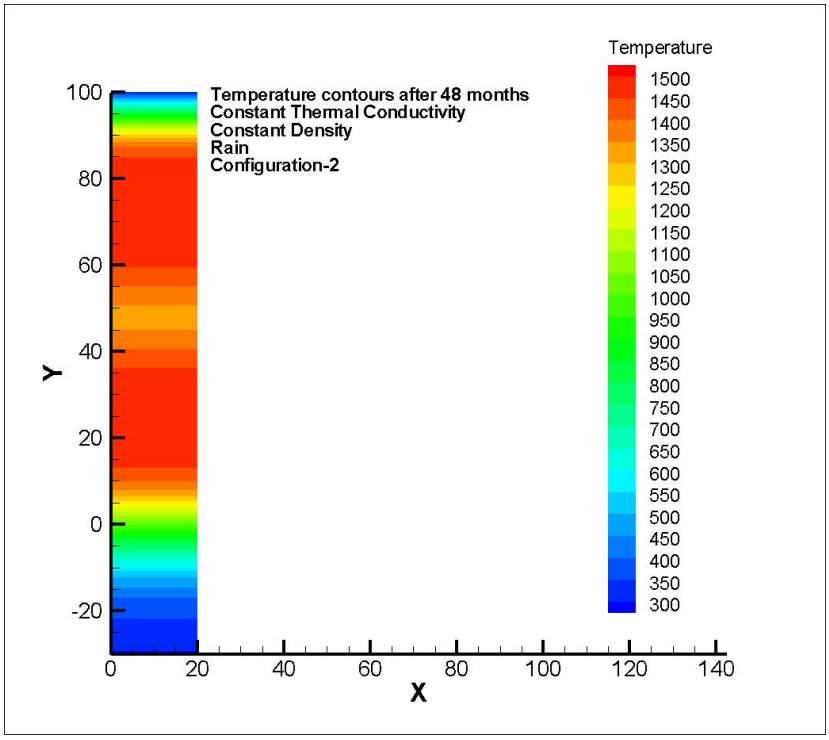

Figure 3-37. Temperature Distribution for the Second Configuration After 48 Months

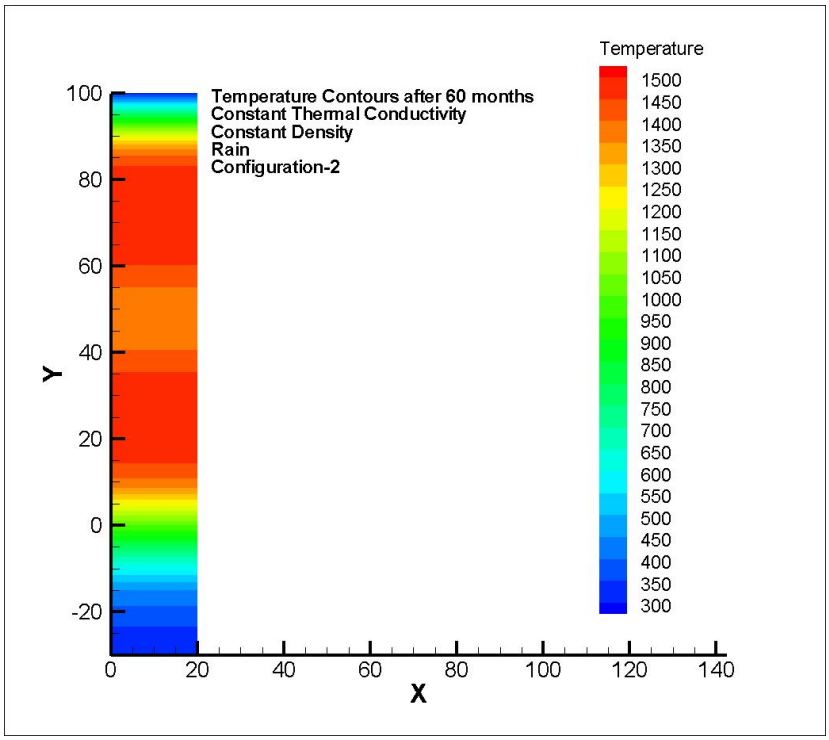

Figure 3-38. Temperature Distribution for the Second Configuration After 60 Months

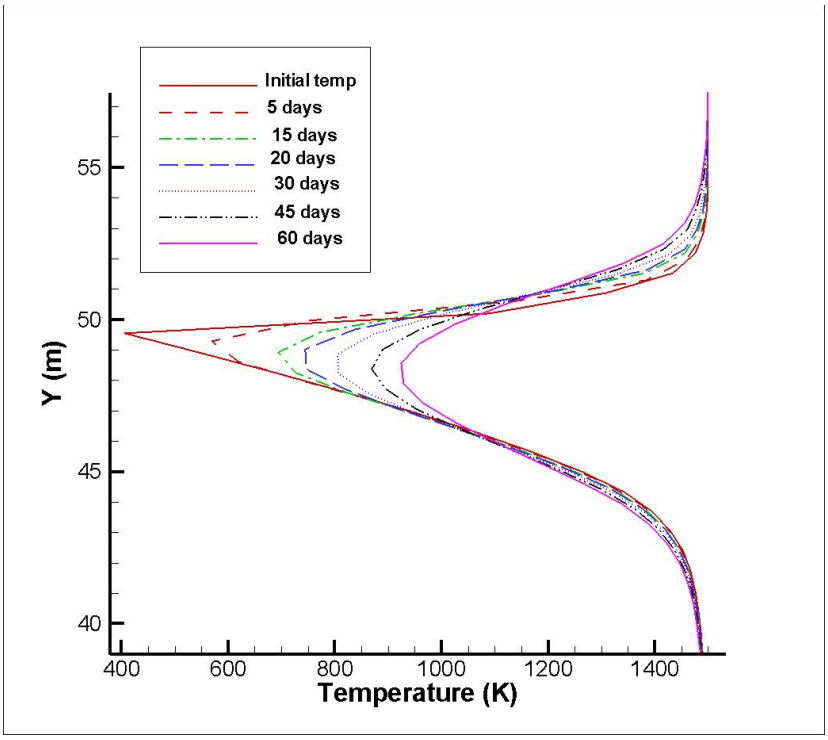

Figure 3-39. Variation of Internal Temperature Gradient Over the First 60 Days of Cooling: Temperature Distribution in the Intersection of the Two Lobes for the Second Configuration

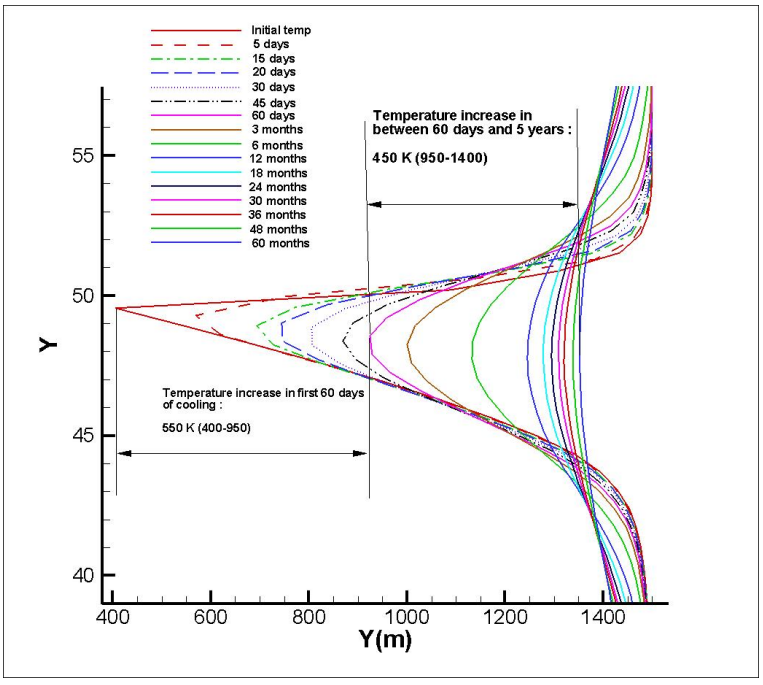

Figure 3-40. Variation of Internal Temperature Gradient Over 5 Years (60 Months) of Cooling: Temperature Distribution in the Intersection of the Two Lobes for the Second Configuration

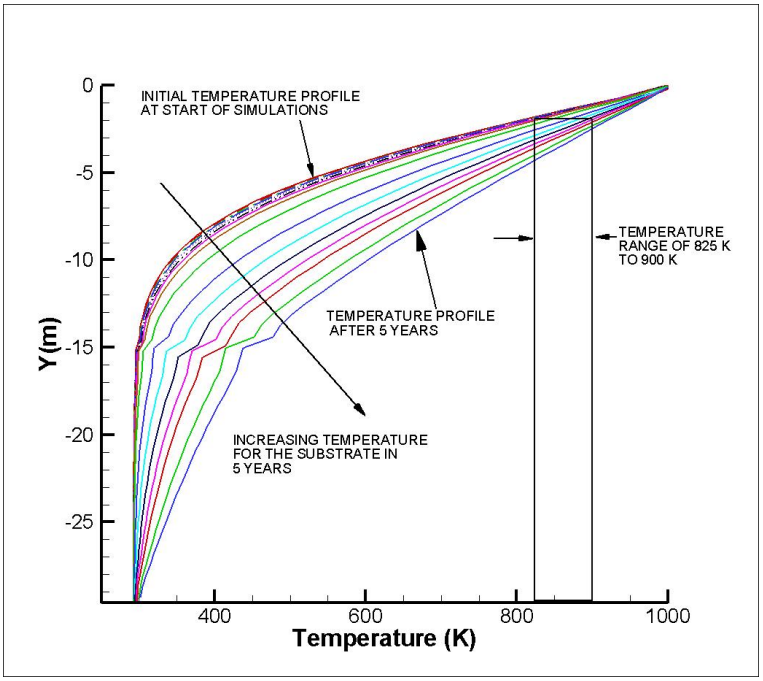

Figure 3-41. Variation of Internal Temperature Gradient Over 5 Years of Cooling: Temperature Distribution Substrate and the Lower Crust for the Second Configuration

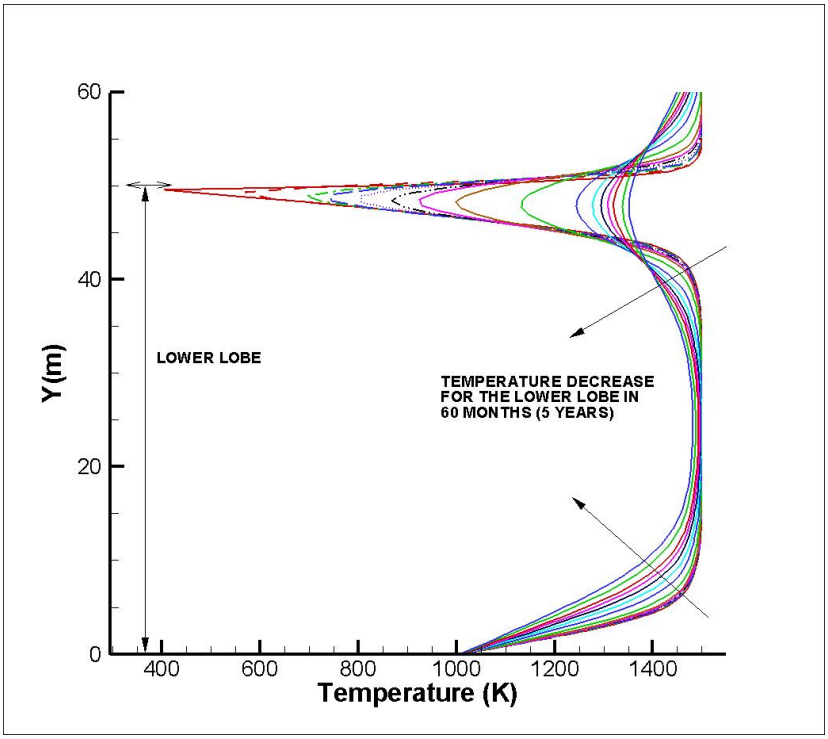

Figure 3-42. Variation of Internal Temperature Gradient Over 5 Years of Cooling: Temperature Distribution in the Lower Lobe for the Second Configuration

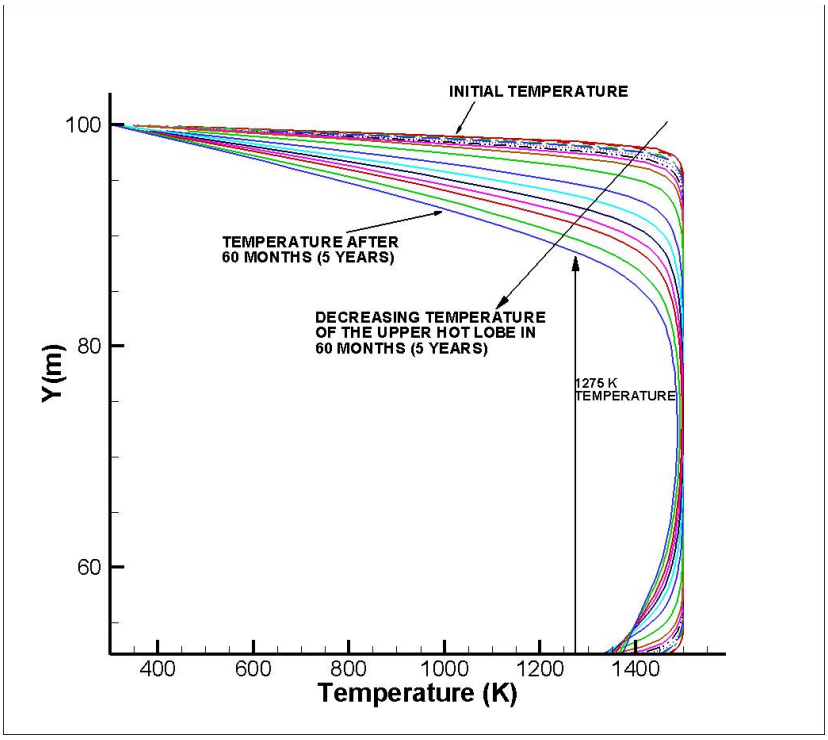

Figure 3-43. Variation of Internal Temperature Gradient Over 5 Years of Cooling: Temperature Distribution in the Upper Lobe for the Second Configuration

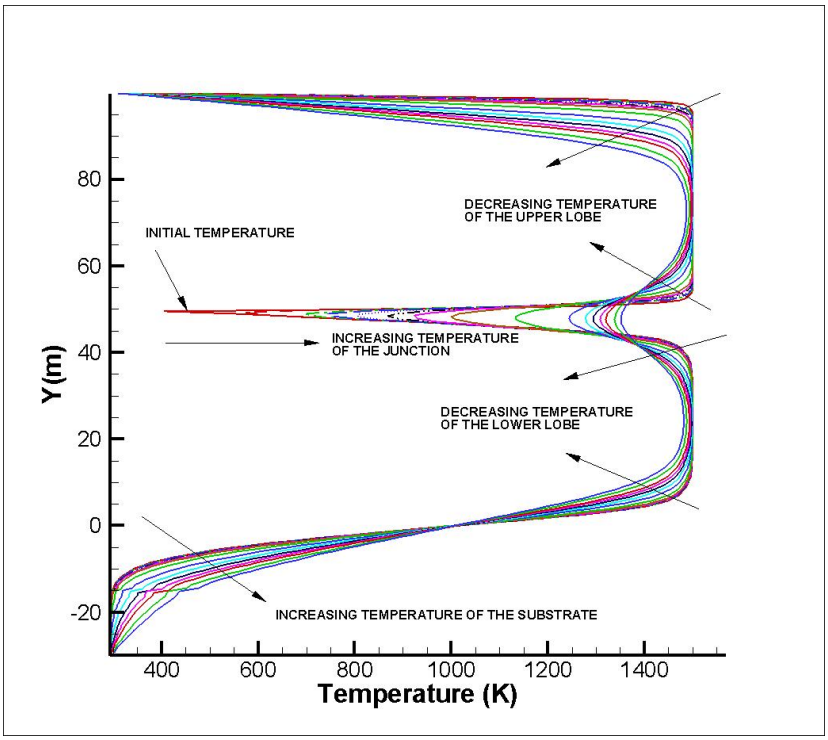

Figure 3-44. Variation of Internal Temperature Gradient Over 5 Years of Cooling: Temperature Distribution Over the Whole Region for the Second Configuration

smaller increase of 60 K [108 °F] in temperature. Similar observations are made in the temperature profiles from the first configuration.

The increase in the temperature of the interface region over 5 years for this second configuration {980 K [1,764 °F]} is comparable to the increase in the temperature of the interface region over 5 years for the first configuration. On close observation, one can see that the initial minimum temperature is not at 50 m [164 ft], but somewhat lower at 49.75 m [163.2 ft]. In addition, the minimum temperature shown in this plot is around 430 K [314 °F], which is higher than 300 K [80.3 °F] (the initial temperature of the intersection). This discrepancy can be attributed to numerical errors and mesh quality. The computational grid used in these simulations is unable to capture the exact temperature change in the interface region. A very fine grid clustered near the intersection would have been able to predict exactly 300 K [80.3 °F] at 50 m [164 ft] (interface between top and bottom lobes). It can also be observed that the nature of the temperature decrease in the upper lobe's bottom 10 m [32 ft] is different from the temperature decrease in the lower lobe. Comparing Figure 3-40 with Figure 3-18, one can see that this difference is more prominent in the second configuration (Figure 3-40) than the first configuration.

Figure 3-41 shows the enlarged view of the bottom lobe's contact with the solidified lava substrate and ground region below, and the variation of the internal temperature gradient through the substrate. It can be observed that the temperature in this region increases by approximately 300 K [540 °F] over the 5-year period. This is expected because the heat flux from the interface region is conducted down to the bottom lobe region and consequently there is a temperature increase in this region. Also, this range of increase {300 K [540 °F] in a 5-year period} for the second configuration is greater than the range of temperature increase observed for the first configuration, because the second configuration has a lower initial temperature at the top of the lobe. Comparing with Figure 3-19, one can observe that the initial temperature for the first configuration is hotter at any depth because the lower lobe is exposed for 1 year before the simulations started, but the temperature difference doesn't increase substantially over the first configuration. This is primarily because rock is a poor conductor of heat. This shows that the temperature increase of the interface region, as well as the temperature increase of the lava substrate is influenced by the initial temperature. Note that the lower lobe is both older and cooler in the second configuration.

Figure 3-42 shows the enlarged view of the lower lobe and the temperature variation across the lower lobe for 5 years. The temperature in the lower as well as in the upper part of the lower lobe decreases by almost 200 K [360 °F] over the 5-year period. While the temperature of the solidified lava substrate and ground increases with time, the temperature of the lower lobe decreases with time and reaches a thermal equilibrium with the solidified lava substrate.

Figure 3-43 shows a similar enlarged view of the upper portion of the top lobe and the variation of the internal temperature gradient across the region. An almost 300 K [540 °F] temperature reduction can be observed for this region. This is because rain and the convective heat transfer cool the upper surface. The degree of cooling of the top surface of the upper lobe is same for the first and second configurations because for both these configurations, the top of the upper lobe has the same initial temperature after 1 month of cooling. Figure 3-44 shows the temperature variation across various zones over the 5-year period.

Based on the simulations, the following conclusions can be made for this second configuration. Maximum heating of the top of the lower lobe in the mid-section occurs within the first 3 years and is of the same order as the first configuration {600 K [1,080 °F]}, despite the modeled

12-month-long cooling period for the lower lobe. Temperature change in the mid-section interface region between the two lobes slows down after 3 years and temperature change between 3–5 years is not significant. Below the bottom lobe, the lava substrate and solidified lava is heated by approximately 300 K [540 °F] in 6 years and the temperature change gradient is almost constant over the simulation time/period. The upper crust of the top lobe cools by approximately 300 K [540 °F] in 5 years, again with temperature change gradient almost constant.

3.3 Comparison of the Simulation Results for the Two Configurations

A brief comparison of the two configurations is presented in Figures 3-45 through 3-50. These figures show the temperature distribution variation at the interface region (contact) of the upper and lower lobes, and in the upper and lower lobes at different time intervals. Figure 3-45 compares the initial temperature distribution for the two configurations. For the upper lobe, the temperature distributions for both the configurations are on top of each other. This is expected because in both configurations the top lobe has cooled for 1-month and its cooling is virtually independent of the lower lobe. Progressing through Figures 3-46 through 3-49, one can see the temperature gradient in the lower lobe for the two configurations slowly converging on top of each other. Although the degree of heating is the same for both configurations, the value of the temperature at the interface is lower for the second configuration after cooling. This is because the heating started at a lower temperature. Figure 3-50 shows that the temperature in the lower lobe for the first and the second configurations equilibrates in 5 years. These results are expected and intuitive, but what is surprising is how much of the heat loss is reestablished in the second configuration, despite 12 months of simulated cooling of the lower lobe.

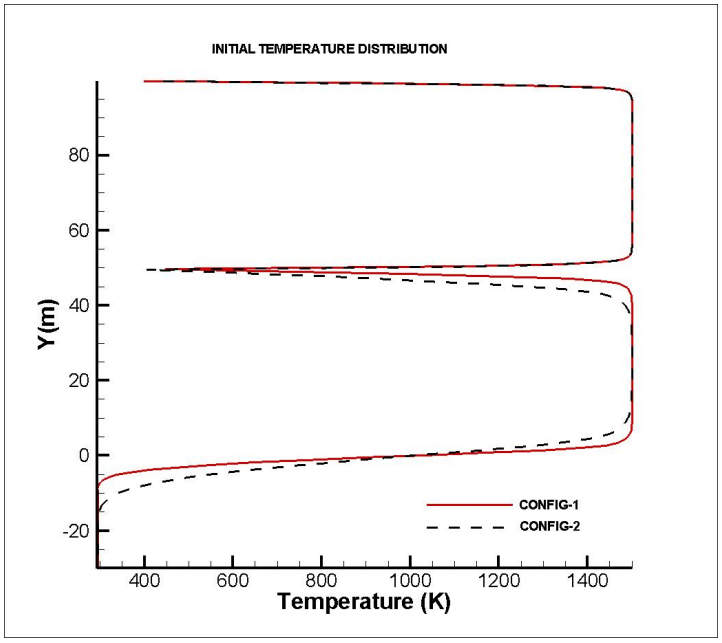

Figure 3-45. Initial Variation of Internal Temperature Gradient: Comparison Between Configurations 1 and 2

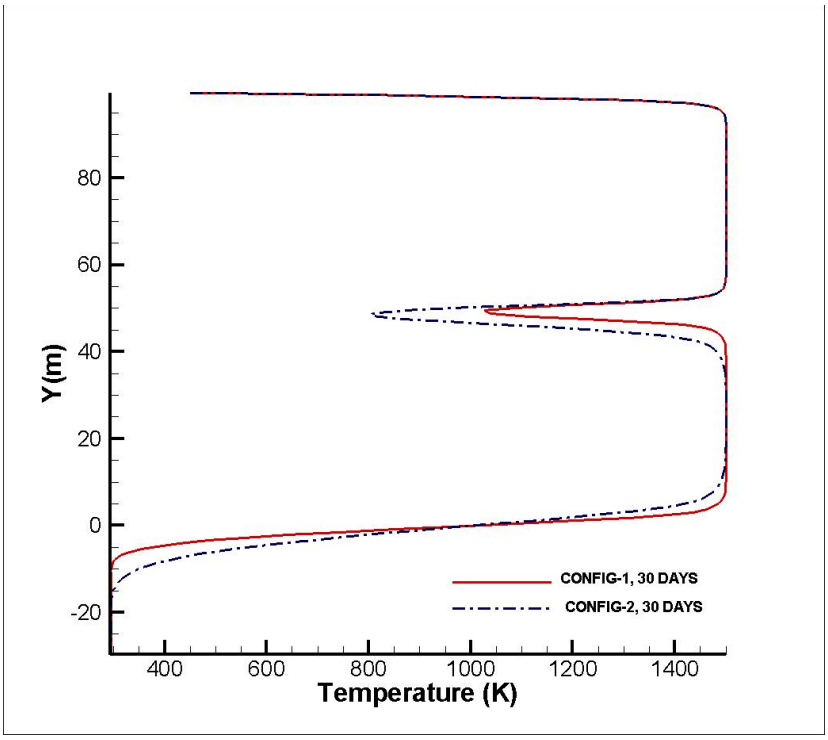

Figure 3-46. Variation of Internal Temperature Gradient After 30 Days of Cooling: Comparison Between Configurations 1 and 2

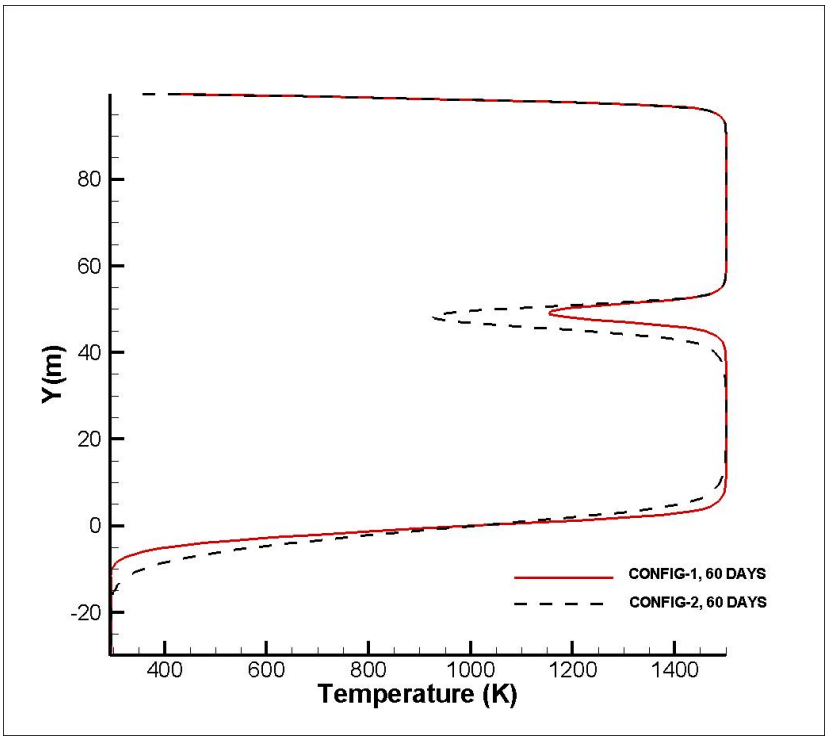

Figure 3-47. Variation of Internal Temperature Gradient After 60 Days of Cooling: Comparison Between Configurations 1 and 2

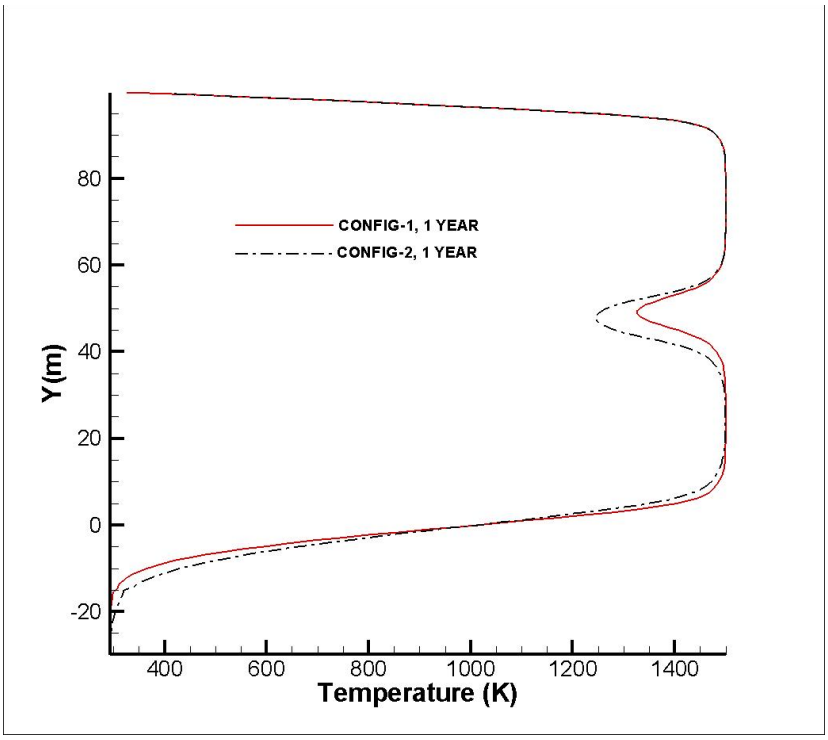

Figure 3-48. Variation of Internal Temperature Gradient After 60 Days of Cooling: Comparison Between Configurations 1 and 2

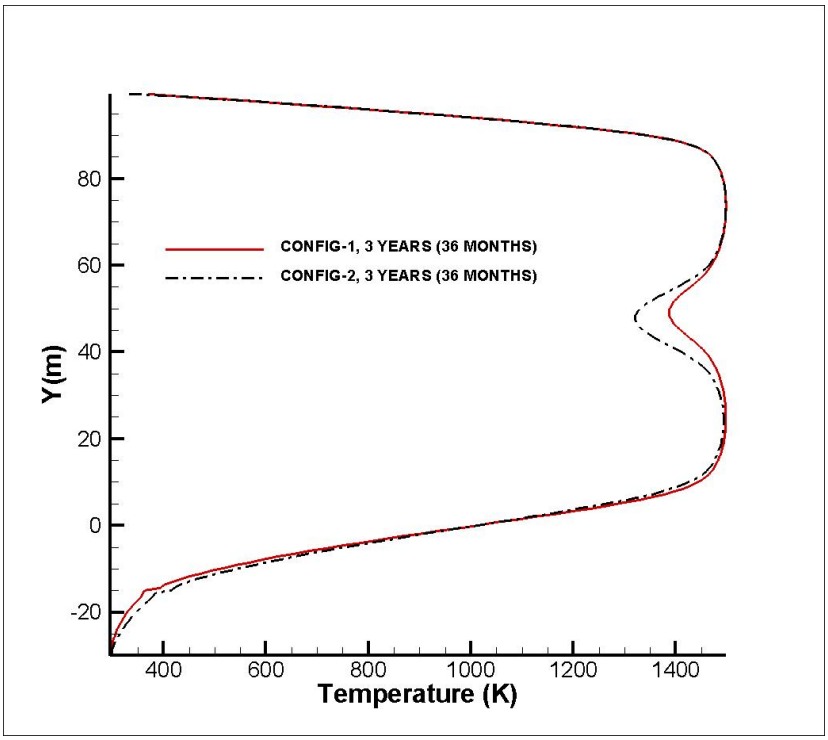

Figure 3-49. Variation of Internal Temperature Gradient After 3 Years of Cooling: Comparison Between Configurations 1 and 2

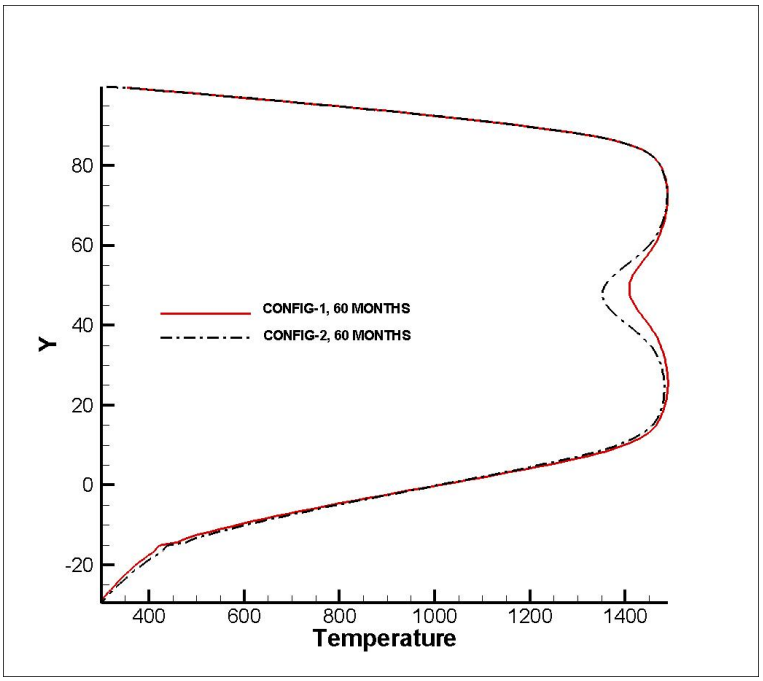

Figure 3-50. Variation of Internal Temperature Gradient After 5 Years of Cooling: Comparison Between Configurations 1 and 2

4 CONCLUSIONS

In the present work, computational modeling was conducted to investigate the cooling pattern when a hot lobe of lava is placed on top of a cooler lobe. Two different configurations have been considered. In the first configuration, the bottom lobe of lava has cooled for 3 months under ambient conditions, while the upper lobe has cooled for 1 month under ambient conditions. In the second configuration, the bottom lobe has cooled for 12 months under ambient atmospheric conditions, while the upper lobe has cooled for 1 month under ambient conditions. The geometric configuration is such that the lower crust of the upper lobe is not considered in the simulations. These numerical simulations provided critical insight into the long-term (~3–5 years) thermal behavior of the whole configuration under natural conditions.

Salient points of these analyses follow.

- Multimode heat transfer takes place from the hotter upper lobe to the cooled lower lobe. From the top surface of the upper lobe, the heat transfer is dominated by convection and radiation, whereas at the interface between the upper and the lower lobes, heat transfer takes place through conduction only.

- Lava temperatures at the top of the lower cooler lobe increase at the contact with the hot lobe. Significant increase in temperature in the mid-section (joint) of the two lobes is observed. However, maximum heating of the top of the lower lobe in the mid-section interface region between the two lobes occurs within the first 3 years. A significant increase in temperature in the mid-section (where the two lobes join together) is observed, even after the lower lobe was allowed to cool for 1 year before the upper lobe was added. What is surprising is how much of the heat loss is reestablished in the second configuration, despite 12 months of simulated cooling of the lower lobe. The 12-month-cooled contact zone reaches at peak temperature that is only 50 K [−90 °F] less than the 3-month-cooled case after 5 years (Figure 3-50).

- Including heat loss from rain does not significantly affect simulation results with constant thermal conductivity and constant density.

- Maximum heating of the top of the lower lobe in the mid-section occurs within the first 3 years. Temperature change between 3–5 years is not significant.

- The initial temperature of the bottom lobe significantly influences the heating pattern of the lower lobe, the solid lava substrate, and the solid ground.

The results presented in this report are preliminary and do not constitute a comprehensive analysis of lava cooling on Earth's surface in a natural environment. However, this analysis takes into account all modes of heat transfer in the computations. This analysis does not include the effect of daily atmospheric temperature variation on the predicted thermal field and temperature, which is expected to be minimal (Keszthelyi and Denlinger, 1996). The temperature patterns inside the cooling lava body provide insight into the cooling and solidification history for basaltic lava lobes on top of each other with a different degree of cooling. This work enhances the observations made from the previous work by Basu, et al. (2012) that focused on cooling of a single lobe of lava. The current analysis also shows that the initial temperature field plays a significant role in the final temperature distribution as well as the solidification pattern. Similar observations were also made in the earlier report (Basu, et al., 2012).

This analysis provides critical insights into the thermal characteristics and temperature history of two hot bodies in contact. This analysis and the results of the simulations can be used to speculate on the accuracy with which the times of lobe emplacement can or cannot be determined from field measurements of temperatures. Similar modeling results can potentially direct sampling plans and sensor networks used to support volcanological field investigation. Potential future applications for this simulation approach include hot waste canisters emplaced in a warm borehole. Though factors such as thermal boundary conditions may differ, deep borehole disposal of nuclear waste may present an analogous situation and the temperature field can have similar characteristics.

5 REFERENCES

ANSYS, Inc. "ANSYS FLUENT Version 14.0, User's Guide." Canonsburg, Pennsylvania: ANSYS, Inc. 2011.

_____. "ANSYS FLUENT Version 12.1, User's Guide." Canonsburg, Pennsylvania: ANSYS, Inc. 2009.

Basu, D., K. Das, and S. Self. "Numerical Simulations and Analysis of Lava Flow Cooling." San Antonio, Texas: Center for Nuclear Waste Regulatory Analyses. February 2012.

Burkhard, D.J.M. "Thermal Interaction Between Lava Lobes." *Bulletin of Volcanology*. Vol. 65. pp. 136–143. 2003.

Crisp, J. and S. Baloga. "A Model for Lava Flows With Two Thermal Components." *Journal of Geophysical Research.* Vol. 95. pp. 1,255–1,270. 1990.

Dragoni, M. "A Dynamical Model of Lava Flows Cooling by Radiation." *Bulletin of Volcanology*. Vol. 51. pp. 88–95. 1989.

Gresho, P.M., R.L. Lee, and R.L. Sani. "On the Time-Dependent Solution of the Incompressible Navier-Stokes Equations in Two and Three Dimensions." *Recent Advances in Numerical Methods in Fluids*. C. Taylor and K. Morgan, eds. Swansea, United Kingdom: Pine Ridge Press. 1980.

Head, J.W. and L. Wilson. "Volcanic Processes and Landforms on Venus: Theory, Predictions and Observations." *Journal of Geophysical Research*. Vol. 91. pp. 9,407–9,446. 1986.

Hon, K., J. Kauahikaua, R. Denlinger, and K. Mackay. "Emplacement and Inflation of Pahoehoe Sheet Flows: Observations and Measurements of Active Lava Flows on Kilauea Volcano, Hawaii." *Geological Society of America Bulletin*. Vol. 106. pp. 351–370. 1994.

Ishihara, K., M. Iguchi, and K. Kamo. "Numerical Simulation of Lava Flows on Some Volcanoes in Japan, in Lava Flows and Domes: Emplacement Mechanisms and Hazard Implications." J.H. Fink, ed. *IAVCEI Proceedings in Volcanology*. Vol. 2. pp. 174–207. 1990.

Keszthelyi, L.P. "Rate of Solidification of Silicate Melts on the Earth, Moon, Mars, and Beyond." Proceedings of the 43rd Lunar and Planetary Sciences Conference, Woodlands, Texas, March 19–23, 2012. Houston, Texas: Lunar and Planetary Institute. 2012.

Keszthelyi, L. and R. Denlinger. "The Initial Cooling of Pahoehoe Flow Lobes." *Bulletin of Volcanology*. Vol. 58. pp. 5–18. 1996.

Keszthelyi, L.A., J.L. Harris, and J. Dehn. "Observations of the Effect of Wind on the Cooling of Active Lava Flows." *Geophysical Research Letters.* Vol. 30, No. 19. 2003.

Neri, A. "A Local Heat Transfer Analysis of Lava Cooling in the Atmosphere: Application to Thermal Diffusion-Dominated Lava Flows." *Journal of Volcanology and Geothermal Research*. Vol. 81. pp. 215–243. 1998.

Patrick, M.R., J. Dehn, and K. Dean. "Numerical Modeling of Lava Flow Cooling Applied to the 1997 Okmok Eruption: Approach and Analysis." *Journal of Geophysical Research.* Vol. 109. B03202, DOI: 10.1029/2003JB002537. 2004.

Peck, D.L., M.S. Hamilton, and H.R. Shaw. "Numerical Analysis of Lava Lake Cooling Models: Part II, Application to Alae Lava Lake, Hawaii." *American Journal of Science.* Vol. 277. pp. 415–437. 1977.

Shaw, H.R., M.S. Hamilton, and D.L. Peck. "Numerical Analysis of Lava Lake Cooling Models: Part I, Description of the Method." *American Journal of Science*. Vol. 277. pp. 384–414. 1977.

Van Doormal, J.P. and G.D. Raithby. "Enhancements of the SIMPLE Method for Predicting Incompressible Fluid Flows." *Numerical Heat Transfer*. Vol. 7. pp. 147–163. 1984.

Van Leer, B. "Toward the Ultimate Conservative Difference Scheme IV—A Second Order Sequel to Gudonov's Method." *Journal of Computational Physics*. Vol. 32. pp. 101–136. 1979.

Wooster, M.J., R. Wright, S. Blake, and D.A. Rothery. "Cooling Mechanisms and an Approximate Thermal Budget for the 1991–1993 Mount Etna Lava Flow." *Geophysical Research Letters*. Vol. 24. pp. 3,277–3,280. 1997.

Young, P. and G. Wadge. "FLOWFRONT: Simulation of a Lava Flow." *Computers and Geosciences.* Vol. 16. pp. 1,171–1,191. 1990.